coatings

MDPI

Review

Toxicity of Carbon Quantum Dots: Is There a Dark Side Beyond Their Brightness?

Michel Machado da Silva [1,2], Luiz Vieira da Costa Neto [1,2], Matheus de Castro Vieira [1,2], Victória dos Santos Monteiro [1,2], Lesly Y. Guevara Argueta [1,3], Andy J. Taipe Huisa [1,2], Alinne Ayech [1,2], Carmen Costa [1,3], Martin Federico Desimone [4] and José M. Monserrat [1,2,3,*]

1 Institute of Biological Sciences, Federal University of Rio Grande (FURG), Av. Itália km 8, Rio Grande 96203-900, RS, Brazil; smith-silvamichel@hotmail.com (M.M.d.S.); luizn0806@gmail.com (L.V.d.C.N.); matheusdcvieira@gmail.com (M.d.C.V.); vicdosantosmonteiro@gmail.com (V.d.S.M.); guevaralesly669@gmail.com (L.Y.G.A.); andyjth1792@gmail.com (A.J.T.H.); alinneayech@gmail.com (A.A.); carmen.costa.25@outlook.com (C.C.)
2 Programa de Pós-Graduação em Ciências Fisiológicas, Instituto de Ciências Biológicas (ICB), Federal University of Rio Grande (FURG), Rio Grande 96203-900, RS, Brazil
3 Programa de Pós-Graduação em Aquicultura, Instituto of Oceanografia (IO), Federal University of Rio Grande (FURG), Rio Grande 96203-900, RS, Brazil
4 Instituto de Química y Metabolismo del Fármaco (IQUMEFA), Facultad de Farmacia y Bioquímica, Universidad de Buenos Aires (UBA), Consejo Nacional de Investigaciones Cinetíficas y Tecnicas (COINCET), Buenos Aires 1113, Argentina; martinfdesimone@gmail.com
* Correspondence: josemmonserrat@gmail.com or monserrat_jm@forg.br; Tel.: +55-53-991651192

Abstract

Carbon quantum dots (CQDs) are a diverse group of carbon nanomaterials that have emerged as promising fluorescent nanomaterials owing to their excellent water solubility, photostability, tunable optical properties, and broad applicability in bioimaging, biosensing, drug delivery, and biomedical applications. Several studies have produced and characterized CQDs using biomass through green chemistry. Despite their widespread application, knowledge regarding their in vivo biosafety remains limited, and most statements regarding good their biocompatibility and low toxicity are based on cell bioassays. To address the limited evidence available on this topic, a systematic literature search was conducted in the Web of Science, Scopus, and PubMed databases, identifying 102 eligible studies published between 2014 and 2026. Hydrothermal synthesis is the predominant production method, with purified water (ultrapure, deionized, double-distilled, or distilled) being the most commonly used solvents. Medicinal plants, fruits, vegetables, agro-industrial residues, and algae are the principal carbon precursors. In vivo results show that different animal models (terrestrial vertebrates, fish, and invertebrate species) generally exhibit excellent biocompatibility, with minimal effects on survival, development, morphology, histopathology, and physiological function after exposure to CQDs. The experimental results also showed biodistribution, persistent fluorescence, and remarkable in vivo imaging performances. Other studies have shown the beneficial effects of CQDs, including wound healing, anti-inflammatory activity, tissue regeneration, neuroprotection, and protection against oxidative stress. Studies on the mechanisms of action induced by CQDs are scarce; however, some studies have analyzed the modulation of oxidative stress, antioxidant activity, and inflammatory responses of CQDs. Even when the evidence collected to date seems to indicate very low toxicity or beneficial effects, the question of how green the green synthesis of CQDs remains open and requires not only more toxicological evidence but also life-cycle analyses.

Academic Editors: Baoquan Sun and Yongxiang Leng

Received: 1 August 2026
Revised: 1 September 2026
Accepted: 13 September 2026
Published: 18 September 2026

Keywords: carbon nanomaterials; nanotoxicology; circular economy; bioimaging; antioxidant activity

1. Introduction

1.1. General Introduction

In recent decades, nanotechnology has driven the development of a wide variety of materials at the nanoscale (1–100 nm) with unique physicochemical and electronic properties, offering broad application potential across diverse fields, including biotechnology, diagnostics, and environmental monitoring [1,2]. Within this realm of nanomaterials, fluorescent nanoparticles have garnered significant scientific interest because of their utility in bioimaging [3], biosensing [4], and real-time monitoring of cellular and biological processes [5].

Carbon quantum dots (CQDs) are nanomaterials that were discovered serendipitously during the separation of single-walled carbon nanotubes [6,7]. CQDs often consist of a small carbon framework exhibiting crystalline and/or amorphous characteristics, which confers excellent water solubility. The carbon structures within the CQDs are associated with various functional groups that determine their electrical charges (Figure 1).

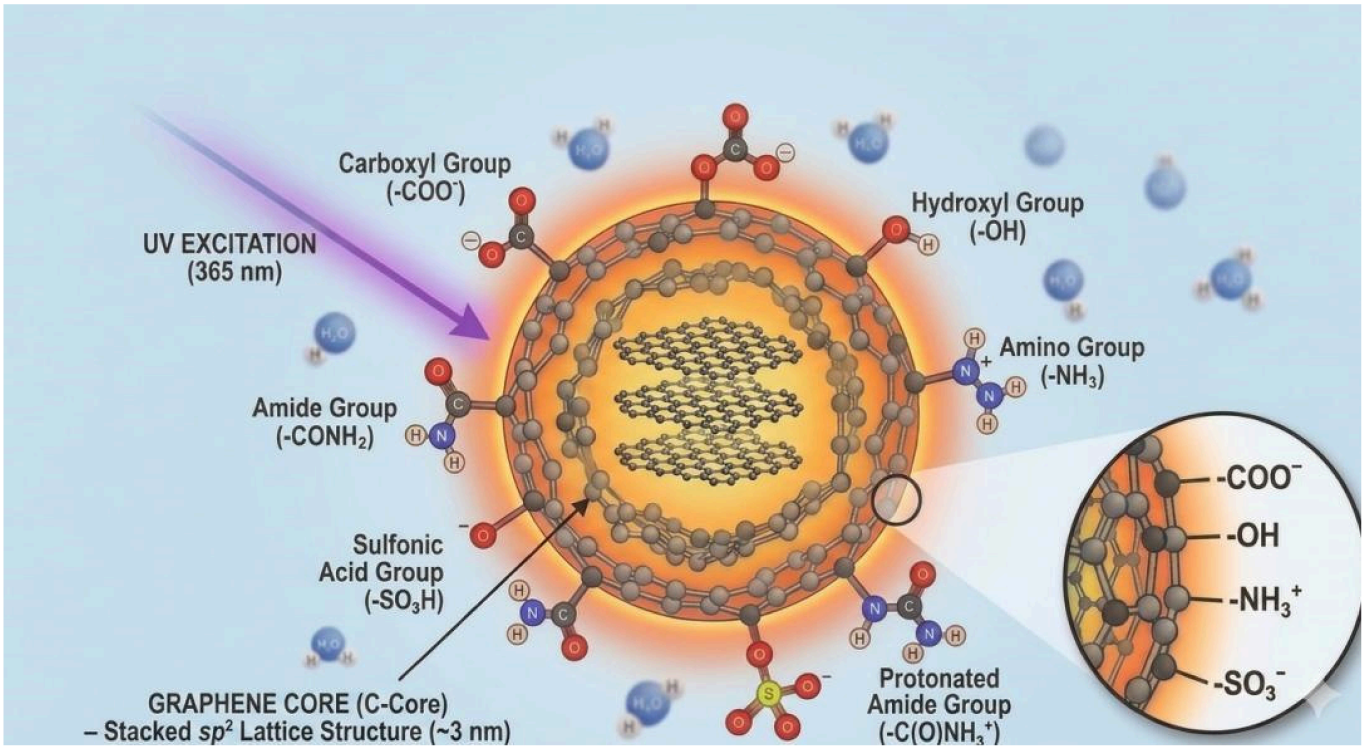

Figure 1. Schematic representation of carbon quantum dots (CQDs), showing the details of the surface functional groups and the central core structure, which in this example is composed of stacked graphene sheets with sp^2 hybridization. Excitation with UV wavelengths induces fluorescence in the CQDs.

One of the most interesting properties of CQDs is their fluorescence emission capability, as quantum confinement causes them to behave like luminescent substances. Al-Raeshedi et al. [8] demonstrated that CQDs synthesized from fruit waste exhibited a Stokes shift of over 170 nm at an excitation wavelength of 340 nm. This shift occurs because the emitted wavelength is longer (and thus lower in energy) owing to the thermal energy dissipated by

the CQDs as they vibrate upon excitation. According to Zhang et al. [9], fluorescence may or may not depend on the CQD core. For instance, if the fluorescence emission remains unchanged despite variations in the excitation wavelength, it is considered evidence that the fluorescence originates from the CQD surface rather than from the core. Furthermore, the fluorescence emission wavelength depends on the CQD size: nanoparticles smaller than 3 nm emit at shorter wavelengths (in the blue range), whereas a redshift—passing through the green wavelength range—is observed for nanoparticles larger than 3 nm [10].

The electrical charge of CQDs is fundamental to their biological activity, as the bactericidal activity of these nanomaterials depends on their electrostatic interactions with negatively charged bacterial cell walls. Studies such as those by Zhao et al. [11] showed that CQDs synthesized from chitosan and ethylenediamine exhibited a higher zeta potential (+20.6 mV) than those generated from chitosan and nitrate, which had a lower zeta potential (+11.7 mV) and a correspondingly lower bactericidal capacity. It should also be noted that CQDs generate reactive oxygen species (ROS), such as hydroxyl radicals (HO•), which exhibit strong bactericidal effects [12]. CQDs can also be used in antimicrobial photodynamic therapy; once internalized by bacteria, they can be excited by light of various wavelengths to generate ROS that are harmful to these microorganisms [12,13].

In addition to their good water solubility, antimicrobial capacity, and fluorescent properties, their low toxicity is also noteworthy, although the vast majority of studies have evaluated only their cytotoxicity [14]. Few studies have assessed the potential in vivo toxicity of CQDs; notable among them is the study by Singh et al. [15], which was conducted on both mice and worms (*Caenorhabditis elegans*). The results indicated that CQDs could be incorporated into worms, enabling visualization without toxicity. CQDs also demonstrated potential for noninvasive bioimaging in mice without causing toxicity. The lack of a critical, organized review of the literature focusing on the potential in vivo toxic effects of CQDs motivated the preparation of this review article.

1.2. Context and Motivation for the Review

Over the years, heavy-metal-based semiconductor quantum dots, such as cadmium telluride (CdTe) and cadmium selenide (CdSe), have been extensively explored because of their optical properties, including high fluorescence efficiency and photostability [16,17]. However, concerns regarding the toxicity of these materials have arisen because of the use of heavy metals with high toxicity potential [18]. Given this scenario, it is important to seek alternative nanomaterials that offer high optical performance and biocompatibility, prioritizing low-toxicity compounds.

In this context, carbon quantum dots (CQDs) have emerged as a class of carbon-based nanomaterials with sizes of less than 10 nm [10,19]. They exhibit high biocompatibility, low toxicity, excellent water solubility, strong light emission (fluorescence), and photochemical stability [20,21]. These characteristics make CQDs favorable for applications in biological systems, contributing to the steady growth of research on their use in bioimaging, biosensing, and diagnostics [22,23]. As research on CQDs has advanced, various synthesis methods have been developed, including top-down and bottom-up approaches, encompassing physical, chemical, and hydrothermal techniques [24]. However, green synthesis is gaining prominence as a sustainable and low-cost approach for producing CQDs. This route involves the use of microalgal biomass [25], plant extracts [26], legumes [19], leafy vegetables [15], and biological waste [27], enabling a reduction in the use of toxic reagents and minimizing environmental impacts compared to traditional methods, while also making the process more cost-effective and less harmful to the environment.

Owing to their beneficial properties, CQDs have attracted significant interest and have been widely investigated for biological and biomedical applications [28]. Notable examples

include cellular and tissue bioimaging [29], biosensor development [30], drug delivery systems and photodynamic therapies [31]. Furthermore, their ability to emit stable fluorescence at various wavelengths, combined with their low toxicity, makes CQDs attractive for both in vitro [32] and in vivo [33,34] applications in diverse experimental models.

Recent studies have shown that most research involving green-synthesized CQDs focuses on in vitro systems utilizing cell lines [35] and Gram-positive and Gram-negative bacteria [36]. However, over the past decade, studies have also been conducted using various in vivo biological models, including aquatic organisms, vertebrates, and invertebrates, such as the fish *Danio rerio* [33,37], the nematode *Caenorhabditis elegans* [19,31], the microcrustacean *Daphnia magna* [38], the fly *Drosophila melanogaster* [39], and rodents [35]. These animal groups allow for the assessment of important parameters such as physiological changes, bioaccumulation, biodistribution, impacts on various organs and tissues, and ROS production [26,31,35,38]. However, the results available in the literature still show discrepancies linked to differences in the synthesis methods, physicochemical characteristics of CQDs, and varying synthesis conditions [10,40]. This lack of standardization hinders the comparison of studies and the understanding of the actual impact of these nanomaterials on organisms in vivo.

Despite advances in the development of CQDs via green synthetic routes, significant challenges remain. The lack of a well-established relationship between physicochemical characteristics and the effects observed in vivo represents a significant gap in the literature on this topic. Furthermore, most studies are conducted in vitro, which hinders the definition of toxicity standards, as these models do not accurately represent the complexity of living organisms and have limited predictive power regarding their in vivo effects [41]. In this context, a critical analysis of the advances and challenges associated with green-synthesized CQDs, focusing on in vivo evidence, is essential to guide the safe and sustainable development of nanomaterials for biomedical applications. As with any emerging nanotechnology, initial research focuses on various applications, while potential human and environmental toxic effects are evaluated later.

To obtain a first glance, a preliminary literature search was conducted on Scopus (www.scopus.com) on 1 April 2026, using three keyword categories: (1) "carbon dots," to estimate the total number of articles published in this field; (2) "carbon dots AND toxicology," to assess information regarding the potential toxic effects of CDs; and (3) "carbon dots AND toxicology AND in vivo," to determine the total number of studies analyzing the systemic toxicity of CDs. As shown in Figure 2, there is a clear imbalance in the types of scientific publications, with toxicology-related studies being underrepresented; articles evaluating toxicological aspects and those assessing in vivo toxicological responses account for only 0.35% and 0.09% of the total published literature, respectively.

Given the scarcity of information, this review aims to critically analyze studies on CDs obtained via green synthesis, focusing on in vivo studies. This study aimed to associate physicochemical properties with observed biological responses, thereby contributing to a better understanding of their biosafety and the development of environmentally friendly nanomaterials for various applications.

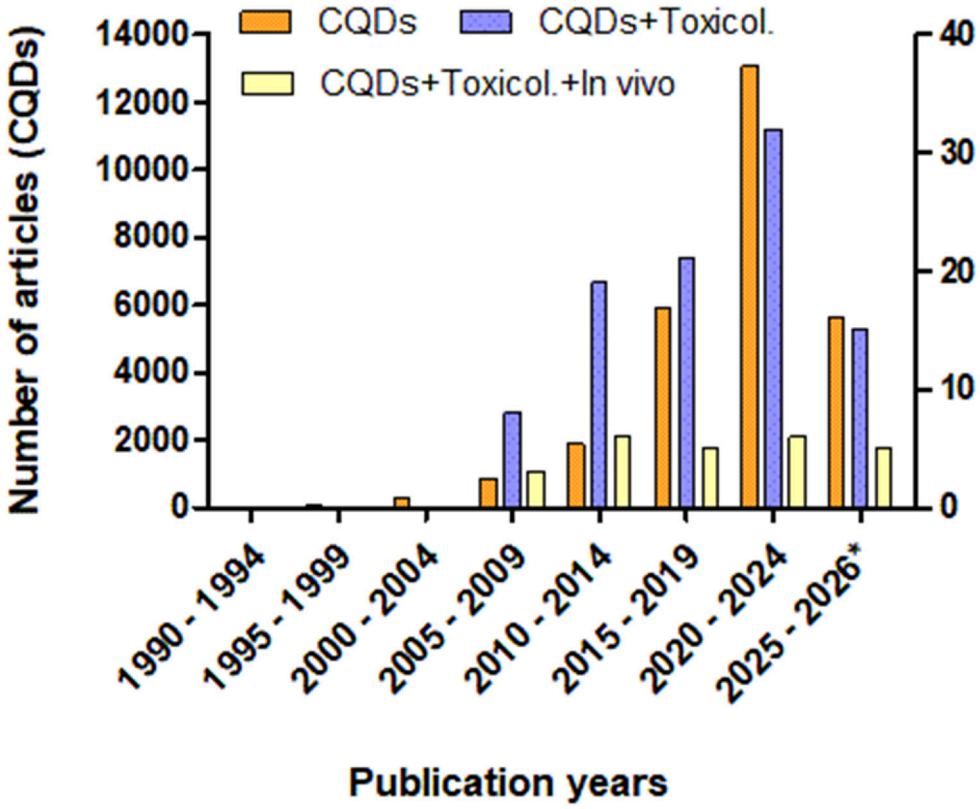

Figure 2. Number of articles found in the Scopus database (www.scopus.com) using the following keywords: (1) "carbon quantum dots" (orange); (2) "carbon quantum dots AND toxicology" (blue); and (3) "carbon quantum dots AND toxicology AND in vivo" (yellow). The left *y*-axis shows the number of articles found using keywords (1). The right *y*-axis shows the number of articles found using keywords (2) and (3). Note: The * refers to Figure S1 in Supplementary Information.

2. Materials and Methods

A systematic literature search was performed using the following terms:

("green synthesis" OR biosynthesis OR biogenic OR biobased OR "bio-based" OR biomass OR fruit OR "food-derived" OR ecofriendly OR "eco-friendly" OR sustainable OR "plant-mediated" OR "biomass-derived" OR natural) AND ("carbon dots" OR "carbon quantum dots" OR CQDs) AND ("in vivo" OR fish OR zebrafish OR mice OR mouse OR rat OR Daphnia OR "*Caenorhabditis elegans*" OR "animal model" OR biodistribution) AND (toxicity OR toxicological OR safety OR biocompatibility OR biosafety OR imaging OR therapeutic OR therapy) NOT ("CdSe quantum dots" OR "cadmium quantum dots").

This string was used as a search strategy in the Web of Science, Scopus, and PubMed databases on 15 May 2026. After applying the criteria established in the three databases, 869 articles were identified for review. From this initial number, duplicate studies were removed, resulting in 488 articles. After screening the titles, abstracts, and keywords, 120 articles were selected for full-text assessment. Finally, after full-text evaluation, 102 articles were included in this review. The included studies were published between 2014 and 2026 (Figure S1). The exclusion criteria were as follows: (i) studies in which the biological effects of CQDs were evaluated using models other than in vivo animal models, such as plants, ex vivo, or in vitro models; (ii) studies in which the carbon source used for CQD synthesis was not derived from plants, microalgae, microorganisms, waste, or residues; and (iii) studies in which the carbon precursor was an isolated or purified compound obtained from any of the aforementioned biological sources. Doping, surface functionalization, coating, or conjugation with drugs or other hybrid components were not

used as exclusion criteria at this stage; these formulations were retained and subsequently classified (Table S1, Supplementary Materials).

In this survey, a material was classified as a carbon quantum dot (CQD) when the original study described it using any of the terminological variants currently applied to this class of material (e.g., carbon dots, carbon quantum dots, CQDs) present in the search terms, and it then went through the eligibility and exclusion criteria (Figure S1).

Bibliometric data were analyzed using VOSviewer software (1.6.21), and a co-occurrence network analysis model was applied to complement the narrative review of the selected studies. Metadata were retrieved from the 102 selected publications, of which 85 contained author keywords and were therefore included in the co-occurrence analysis. The remaining publications did not provide this metadata in the original source and were consequently excluded from this analysis. To facilitate the interpretation of research trends, similar keywords were merged into single terms (e.g., carbon dots and carbon quantum dots). This approach allowed the visualization of keyword co-occurrence patterns and the identification of the main research themes over the last four years.

3. Results

3.1. Bibliometric Overview of the Selected Studies

The bibliometric analysis identified three main research themes: (I) carbon dot synthesis and characterization, (II) biomedical applications, and (III) biological mechanisms related to oxidative stress and inflammation. The bubble size is proportional to the frequency of occurrence of each term, and the link thickness reflects the strength of the association between the terms. Among the most frequently associated keywords were bioimaging, wound healing, biocompatibility, and hydrothermal, indicating that a substantial proportion of the literature focuses on the synthesis strategies, material characterization, and biomedical applications of CQDs. In contrast, terms related to mechanistic investigations, such as nanozyme and reactive oxygen species, showed fewer occurrences and connectivity within the network (Figure 3A). Although antioxidant activity has emerged as a recent research trend, most studies have focused on demonstrating biological effects, whereas comparatively fewer studies have investigated the molecular mechanisms underlying these responses (Figure 3B). Overall, the bibliometric analysis outlines the current research landscape and provides a conceptual framework for the subsequent sections, in which the available evidence is critically discussed according to synthesis approaches, psychochemical properties, biological applications, and molecular mechanisms.

3.2. Important Characteristics of the Green Synthesis Process for CQDs

3.2.1. Types of Synthesis Methods and Used Solvents

Figure 4A shows the distribution of the synthesis methods employed in the studies included in this review. Hydrothermal synthesis was the most frequently used technique for obtaining CQDs, accounting for 56% of the analyzed articles in this review. Microwave-assisted synthesis, the solvothermal method, and pyrolysis followed similar frequencies, each representing approximately 9% of the total studies. Hydrothermal carbonization was the least frequently used method, comprising 8% of the selected studies. Overall, hydrothermal synthesis was the predominant synthesis route identified in the literature. Regarding the solvents used in the synthesis processes, Figure 4B shows a clear predominance of purified water—whether ultrapure, deionized, double-distilled, or distilled—with 76% of the analyzed studies using purified water as a solvent.

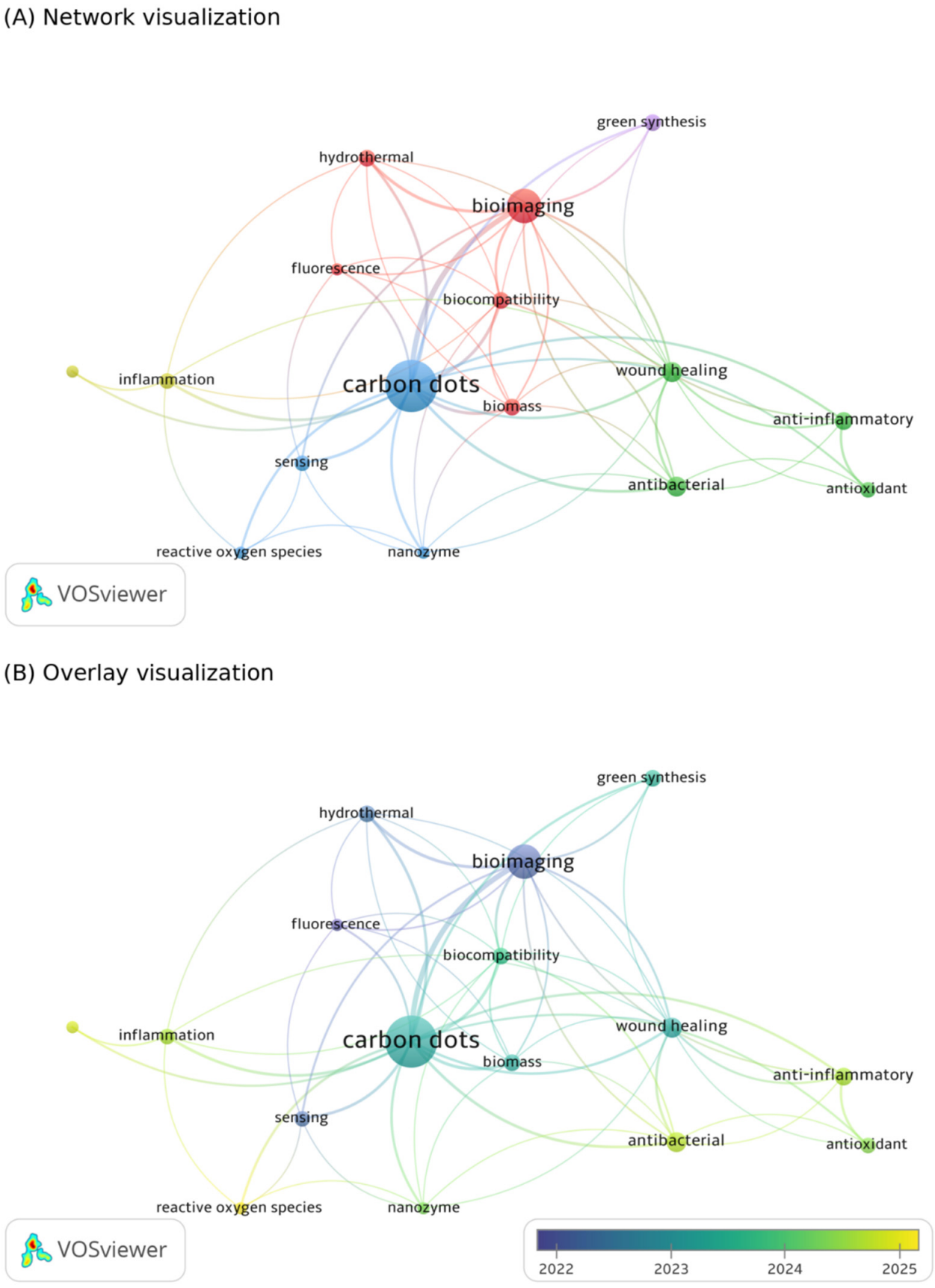

Figure 3. Bibliometric analysis of the author's keywords. (**A**) Network visualization showing keyword co-occurrence and link strength. (**B**) Overlay visualization showing the average publication year of each keyword, where blue indicates older topics and yellow indicates more recent topics.

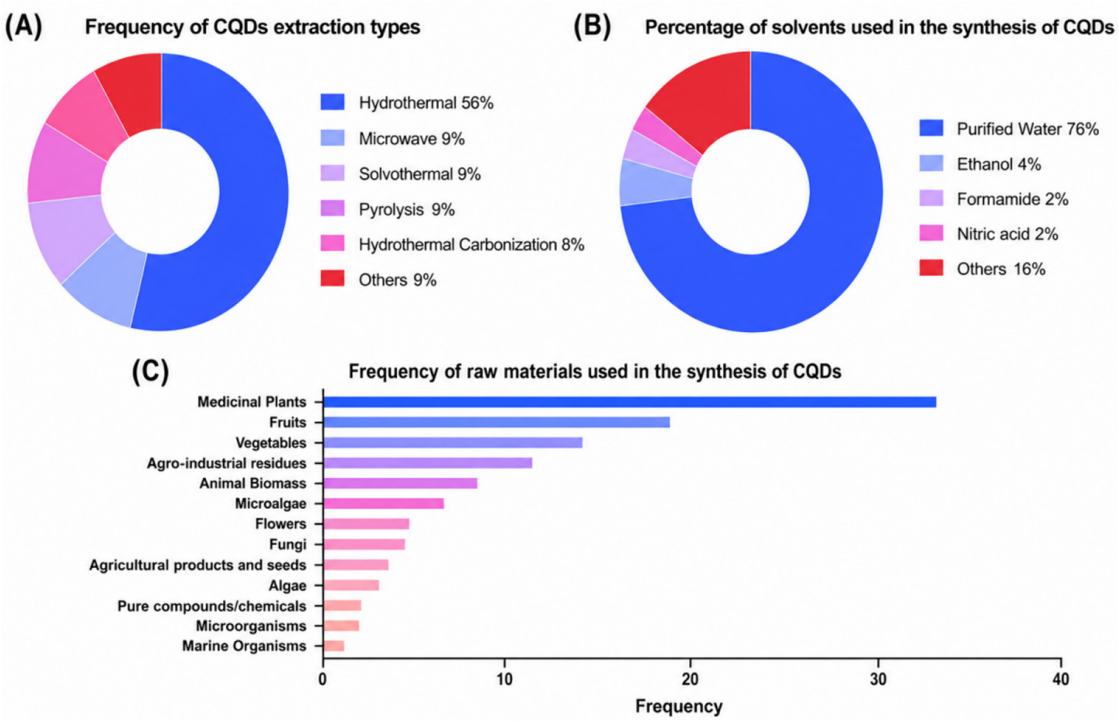

Figure 4. Overview of the synthesis methods, raw materials, and solvents used for synthesizing carbon quantum dots (CQDs). (**A**) Distribution of CQD synthesis methods, showing hydrothermal synthesis as the most widely used approach (56% of the total studies). (**B**) Distribution of solvents used in CQD synthesis, with purified water (including deionized, distilled, and ultrapure water) accounting for 76% of the studies. (**C**) Frequency of raw materials employed, highlighting medicinal plants as the predominant source of raw materials.

3.2.2. Raw Materials Used

Precursors from various sources have been identified, including medicinal plants, fruits, vegetables, agro-industrial residues, animal biomass, agricultural products, seeds, flowers, algae, microalgae, fungi, microorganisms, and pure chemical compounds. Among these categories, studies using medicinal plants were the most frequent, followed by those using fruits, agro-industrial residues, and vegetables (Figure 4C).

3.2.3. Extraction Time, Purification Processes, and Temperature Used for CQDs Synthesis

Figure 5A shows the distribution of extraction times in the studies included in this review. Times ranged from less than 1 h to 24 h, with 4, 12, and 24 h being the most frequently reported. Intermediate times, such as 8 h and 16 h, were less frequently observed. The temperature values ranged from 40 to 500 °C, with 200 °C being the most reported experimental condition. Temperatures between 150 and 250 °C were also observed, whereas temperatures above 300 °C were less frequent (Figure 5B).

Studies have documented the use of dialysis and filtration membranes for purification. For dialysis membranes, different molecular weight cut-offs (MWCO) were used, ranging from 1 to 14 kDa. Membranes with a 1 kDa cut-off were the most common in the evaluated studies, followed by membranes with a 3.5 kDa MWCO (Figure 5C). In the case of filters, membranes with a pore size of 0.22 µm were predominant, while membranes with pore sizes of 0.20, 0.21, 11, and 40 µm were used less frequently in the analyzed studies (Figure 5D). However, it should be noted that these standard filtration membranes (e.g., 0.22 µm) possess pore sizes significantly larger than CQD dimensions, meaning that their role is limited to removing macro-aggregates rather than isolating quantum dots or removing molecular impurities.

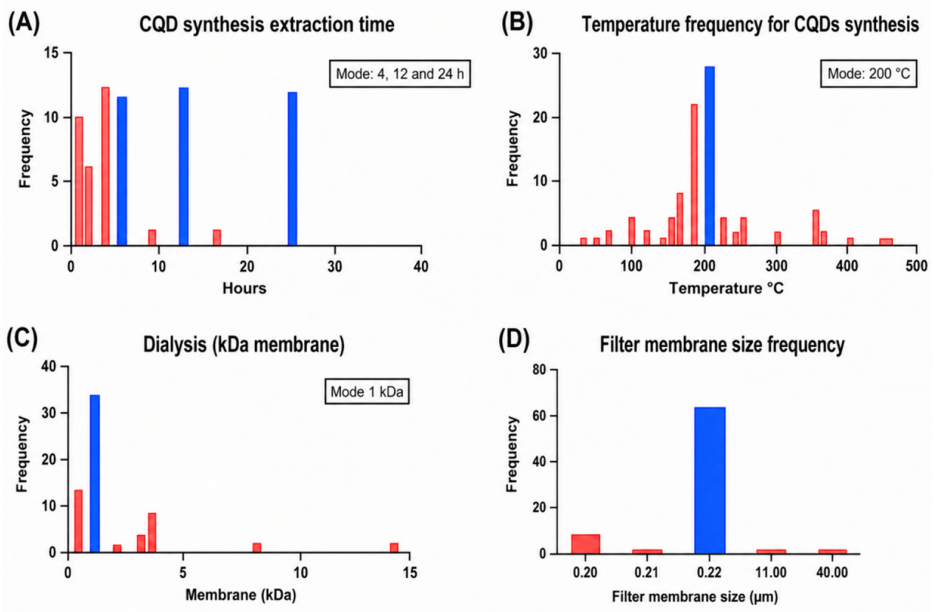

Figure 5. Distribution of synthesis time (**A**), synthesis temperature (**B**), molecular weight cut-offs of the dialysis membranes (**C**), and filtration membrane pore size (**D**) used in the included studies.

3.3. Physicochemical Characterization

3.3.1. Dynamic Light Scattering (DLS)

Table S2 presents the distribution of hydrodynamic diameters obtained via dynamic light scattering (DLS) in the studies included in this review. The values ranged from 0.21 to 552.2 nm, with the highest frequency of particles in the range of up to 10 nm (Table S2 in Supplementary Materials).

3.3.2. Zeta Potential, Quantum Yield and Transmission Electron Microscopy

As shown in Figure 6A, the distribution of zeta potential values in the selected articles ranged from −56.1 to +16.8 mV, with a predominance of negative values. The highest frequency was observed in the −20 to −10 mV range, followed by the −10 to 0 mV and −30 to −20 mV ranges, respectively. Values lower than −40 mV were found in fewer studies, whereas positive zeta potentials were less frequently observed.

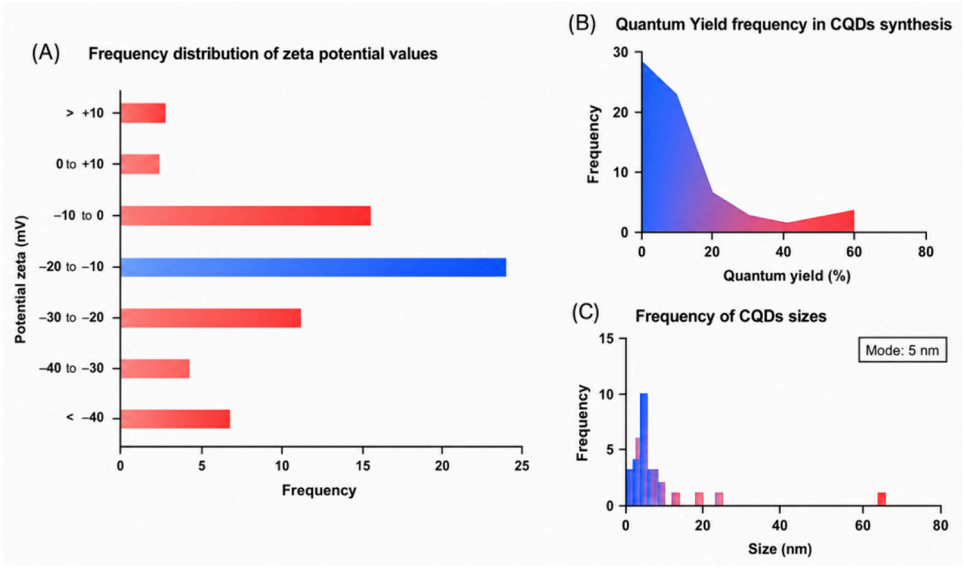

Figure 6. Distribution of the zeta potential (**A**), quantum yield (**B**), and particle size based on Transmission Electron Microscopy (TEM) (**C**) reported in the studies included in this review.

Regarding quantum yield, values ranged from less than 10% to approximately 80%, with the highest frequency of studies showing quantum yields below 10%. The 10%–20% and 20%–30% ranges were also frequently reported, whereas values above 40% were observed in a small number of studies (Figure 6B). Finally, size analyses based on Transmission Electron Microscopy (TEM) results showed that the sizes were mostly between 1 and 10 nm, with a peak frequency at 5 nm (Figure 6C).

3.4. In Vivo Biological Effects of Green-Synthesized CQDs

To facilitate the interpretation of the results of the studies included in this review, the in vivo organisms were grouped according to the biological models used in the articles. The animal models employed in the studies were classified as (1) terrestrial vertebrates (mice, rats, or chickens), (2) fish (*Danio rerio* and *Oryzias latipes*), and (3) invertebrates (*Caenorhabditis elegans*, *Daphnia magna*, and *Drosophila melanogaster*). A total of 109 animal model records were identified across the 102 included articles, as some studies used more than one animal model and were therefore included in multiple categories. Of these, terrestrial vertebrates were used in 62.39% of studies. Fish and invertebrate species accounted for 27.52 and 10.09% of the total species, respectively.

3.4.1. Terrestrial Vertebrates

Mice were the most commonly reported experimental model, accounting for 81% (n = 55) of the studies included in this group (Figure S2A). The most frequently occurring lineages were BALB/c [42,43], C57BL/6 [44,45], C57bl/6J [10,46], Krunming [47,48], Nude [49,50], and Swiss [51,52], all of which have been reported in the literature. Mice accounted for 18% (n = 12) of the studies, represented by the Sprague-Dawley [53,54] and Wistar [55,56] lineages. In addition, only 1% (n = 1) of the studies used chicken *Gallus gallus* as an in vivo biological model [57]. In total, 68 studies involving terrestrial vertebrates were identified (Figure S2B,C).

Biosafety in Terrestrial Vertebrates

In this classification category, studies investigating histopathological changes, serum biochemistry, and other toxicity indicators, including genotoxicity, body weight, and survival were considered. As shown in Figure 7A and Table S3 (Supplementary Materials), studies assessed biochemical markers [57], toxicity indicators, including body weight, genotoxicity, and survival [28,58], and histopathology is the most frequently used endpoint [10,42,59]. Taken together, these results provide important evidence for the assessment of the good biocompatibility of CQDs in terrestrial vertebrate models, as most studies did not identify relevant changes in the analyzed parameters.

Bioimaging and Biodistribution in Terrestrial Vertebrates

Other studies have evaluated their applications in bioimaging and in vivo biodistribution. This category included studies assessing in vivo fluorescence, tissue biodistribution, bioaccumulation, and the persistence of the fluorescence signal over time. As shown in Figure 7B and Table S3 (Supplementary Materials), in vivo fluorescence is the most investigated endpoint, showing the ability of CQDs to incorporate into organs and whole organisms and generate an intense fluorescent signal at different wavelengths [49–52,60–63].

Studies that assessed biodistribution in different tissues and organs were recorded less frequently, followed by bioaccumulation in specific regions and persistence of the fluorescent signal for days and weeks, allowing for in vivo tracing of cells and tissues [15,55,56,64–69].

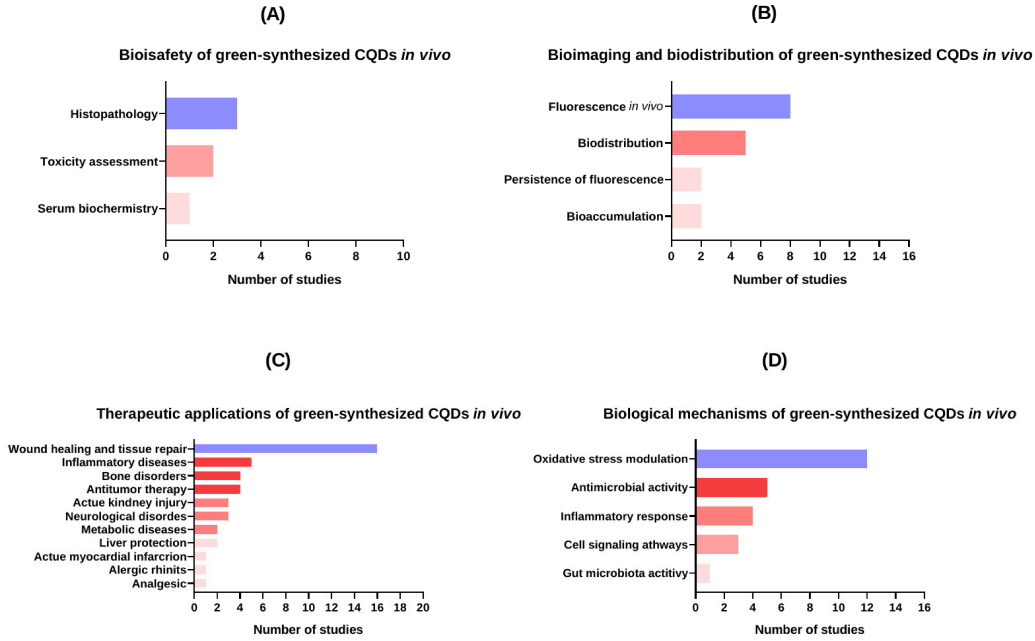

Figure 7. Distribution of the main biological parameters reported in vivo studies in terrestrial vertebrates using green-synthesized carbon quantum dots (CQDs). (**A**) Frequency of biosafety parameters. (**B**) Frequency of evaluation of bioimaging and biodistribution parameters. (**C**) Frequency of therapeutic applications. (**D**) Frequency of biological mechanisms investigated as secondary or tertiary parameters.

Therapeutic Assessment in Terrestrial Vertebrates

For this classification, papers investigating different therapeutic applications, including tissue repair, antitumor therapy, inflammatory diseases, acute renal injury, neurological diseases, metabolic disorders, and other experimental conditions were considered.

As shown in Figure 7C and Table S3 (Supplementary Materials), wound healing and tissue repair were the most frequently investigated therapeutic applications, indicating the potential of CQDs in tissue regeneration in mice and rats of different lineages [43,48,53,70–82].

Highlighted applications include antitumor treatments [43,83–86], therapies for inflammatory diseases [44,45,87–89], bone disorders [90–93], and acute kidney injury models [94–96]. These applications primarily demonstrate effects on tumor growth inhibition, photodynamic therapy, bone regeneration, and modulation of inflammatory responses.

To a lesser extent, CQDs have been investigated in models of central nervous system disease, metabolic disorders, liver protection, protection against acute myocardial infarction, treatment of allergic rhinitis, and analgesia, where treatment with CQDs has promoted specific beneficial therapeutic responses according to the experimental conditions assessed [54,97–105]. These results illustrate the broad therapeutic potential of green synthetic CQDs in terrestrial vertebrate models, particularly mice and rats, with an emphasis on applications aimed at tissue regeneration, controlling inflammation, and treating experimental diseases.

Proposed Mechanisms of Toxicity in Terrestrial Vertebrates

Although few studies have investigated biological mechanisms as a primary objective, several studies in the biosafety and therapeutic evaluation category have used these parameters as secondary outcomes to explain the observed in vivo effects. For this classification, studies evaluating changes related to oxidative stress, inflammatory response, cell signaling pathways, antimicrobial activity, and gut microbiota modulation were considered.

As shown in Figure 7D and Table S4 (Supplementary Materials), oxidative stress modulation was the most frequently reported mechanism. The main results involved the reduction in the production of reactive oxygen species (ROS), malonaldehyde (MDA), and nitric oxide (NO), accompanied by the activity of antioxidant enzymes such as superoxide dismutase (SOD), catalase (CAT), glutathione-S-transferase (GST), and non-enzymatic antioxidants such as reduced glutathione (GSH) and total antioxidant capacity (T-AOC) [44,56,58,70,73,77,83,86,95,99,103,104]. Other mechanisms have been evaluated, including modulation of the inflammatory response characterized by decreased pro-inflammatory cytokines, regulation of cellular signaling pathways such as Wnt/β-catenin, VEGF, TGF-β, MGMT, TLR4/NF-κB, PI3K/AKT, JAK/STAT, antimicrobial activity, and modulation of gut microbiota [45,48,75,79,89,98–100].

3.4.2. Fish

In the studies reviewed, zebrafish was the most commonly reported biological model, accounting for 93% (n = 28) of the studies included in this group (Figure 8A). The most frequently occurring transgenic zebrafish lineages were the AB Wild-type [106,107], Tg (lyz: DSRED2) [70], and CZ59 [87] (Figure 8B). Two other studies were conducted with the Japanese fish *Oryzias latipes*, corresponding to 7% (n = 2) of the included studies [108,109].

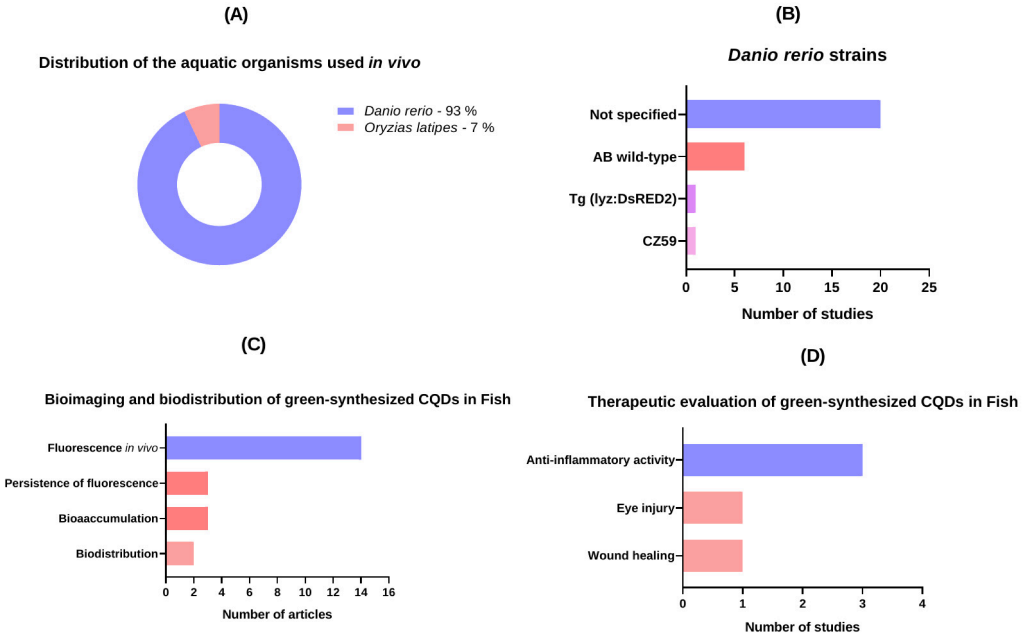

Figure 8. Distribution of key biological parameters reported in vivo fish using green-synthesis carbon quantum dots (CQDs). (**A**) Frequency of biosafety parameters. (**B**) Frequency of *Danio rerio* zebrafish lines used in various studies. (**C**) Frequency of bioimaging and biodistribution parameters. (**D**) Frequency of therapeutic applications.

Biosafety in Fish Species

For this classification, studies investigating histopathological changes and toxicity indicators were included. As presented in Table S3 (Supplementary Materials), histopathology was evaluated in fewer studies, with preservation of organ integrity, including the liver, glands, and skeletal musculature, reported after exposure to CQDs [110]. Toxicological evaluation included endpoints such as behavioral, morphological, and survival paraments [62,111,112].

Bioimaging and Biodistribution in Fish Species

Bioimaging and biodistribution studies investigated the behavior of CQDs after experimental in vivo exposure, including fluorescence, tissue distribution, bioaccumulation, and the persistence of the fluorescence signal. As shown in Figure 8C and Table S3 (Supplementary Materials), in vivo fluorescence was the most investigated endpoint, demonstrating an intense fluorescence signal in embryos, larvae, and adult fish [33,70,90,106–108,113–120]. Other studies have assessed the biodistribution, bioaccumulation, and persistence of fluorescence signals, showing that CQDs can cross biological barriers and distribute into different tissues, independent of the route of exposure [69,109,121–126]. In embryos, this ability has been demonstrated by the permeability of CQDs to the chorion without harmful alterations in larval development [33,108,112,118]. In addition, the maintenance of the fluorescent signal for hours or days and high cellular internalization enhance the potential of CQDs for in vivo bioimaging applications [69,119].

Therapeutic Assessment in Fish

The studies classified in this category considered anti-inflammatory activity, wound healing, tissue repair, and protection against ocular injury. As shown in Figure 8D and Table S3 (Supplementary Materials), anti-inflammatory activity was the endpoint most frequently investigated, including the assessment of inflammatory cytokines (TNF-α, IL-6, NO), neutrophil migration, and inflammatory response induced by CuSO4 [87,94,127]. Other studies have assessed wound healing by evaluating the closure of lesions in the zebrafish caudal fin [128] and protection against oxidative stress-induced ocular injury [129]. Studies have demonstrated the therapeutic potential of green-synthesized CQDs in fish models, particularly in modulating the inflammatory response, tissue regeneration, and protection against oxidative stress-induced damage.

Proposed Mechanisms of Toxicity

In general, fish studies have demonstrated that CQDs have high biocompatibility and potential application as bioimaging probes in fish. However, there is a scarcity of investigations that consider the molecular mechanisms involved in the observed beneficial effects, particularly those involved in cell signalling. Among the mechanisms described, two studies demonstrated the direct antioxidant action of CQDs via the direct scavenging of free radicals [87,94]. Deng et al. [127] reported that CQDs regulate nitric oxide (NO) levels and increase the expression of antioxidant enzymes such as superoxide dismutase (SOD) and glutathione peroxidase 4 (GPX-4), enhancing the cellular antioxidant response. Another proposed antioxidant mechanism is the action of CDs as nanoenzymes, mimicking the activity of antioxidant enzymes and generating a cascade of activities that sequentially remove different ROS, resulting in decreased oxidative stress and, as a physiological consequence, the protection of the ocular tissues [129].

Other studies have demonstrated the modulation of inflammatory activity by reducing pro-inflammatory cytokines, such as TNF-α and IL-6, and by increasing the expression of CD206, a marker of repair macrophages, promoting tissue regeneration [87]. In *Oryzias latipes* embryos, the preferential accumulation of CQDs in inflamed cells was due to the high intracellular levels of reactive oxygen species (ROS), favoring their localized antioxidant action [108].

3.4.3. Invertebrates

Parameters Evaluated

The nematode *Caenorhabditis elegans* was the primary invertebrate model used to evaluate the in vivo effects of the CQDs. The most frequently investigated endpoints in-

cluded bioimaging and fluorescence applications, life-history traits (viability, survival, and mortality), behavioral responses (locomotion and body bending), morphological and developmental changes, and cellular and molecular responses, particularly apoptosis-related pathways assessed using mutant strains and gene expression analyses [15,19,26,130–135]. Exposure concentrations ranged from 25 to 1500 μg/mL, although most studies evaluated concentrations between 0 and 250 μg/mL. Bioimaging and fluorescence are the most common applications, emphasizing the widespread use of *C. elegans* as an in vivo model for evaluating the imaging performance and safety of CQDs. The main endpoints evaluated in invertebrate models, along with their associated parameters and representative studies, are summarized in Table S3 (Supplementary Materials).

In addition to *C. elegans*, only two other invertebrate models have been identified so far. In *Daphnia magna*, acute toxicity was evaluated using an immobility assay, whereas *Drosophila melanogaster* was used to investigate survival, behavior, morphology, intestinal cytotoxicity, and bioimaging [38,136].

Main Toxicological Outcomes

Overall, CQDs exhibited excellent biocompatibility with *C. elegans*. Most studies reported survival and viability above 90%–97%, with no significant effects on locomotion, body morphology, growth, or development, even at relatively high exposure concentrations [130,131,134]. At the same time, CQDs display strong, stable, multicolor fluorescence and are readily internalized, primarily through the gastrointestinal tract, allowing the tracking of their distribution throughout the organism and supporting their application as efficient in vivo imaging probes [15,131,134]. Only one study reported a marked biological response to the treatment. Elsherbiny et al. [19] demonstrated that a specific CQDs formulation induced DNA damage-mediated germline apoptosis through activation of the cep-1/p53 pathway, accompanied by increased apoptotic germ cells and egl-1 upregulation in *C. elegans*. However, this response occurred under photodynamic therapy conditions and was intentionally exploited for therapeutic purposes, rather than representing intrinsic nanomaterial toxicity.

In *D. magna*, no immobilization was observed after 48 h of exposure, even at concentrations up to 1000 mg/L, indicating negligible acute toxicity [38]. Similarly, CQDs have demonstrated good biocompatibility with *D. melanogaster*. No significant alterations in morphology, intestinal cell viability, or development were observed in this study. Mild behavioral changes and a slight reduction in survival were observed only for cysteamine-modified CQDs at the highest concentration tested (500 μg/mL). Importantly, the bioimaging application was demonstrated at 250 μg/mL, a concentration at which no relevant toxic effects have been reported [136].

Proposed Mechanisms of Toxicity in Invertebrates

Mechanistic evidence remains scarce, as only a few studies have investigated the biological processes underlying the effects of CQDs. In *C. elegans*, CQDs are efficiently internalized through the digestive tract and distributed throughout the organism, facilitating their use in biodistribution and fluorescence imaging studies [15]. Their high water solubility and abundance of hydroxyl, carbonyl, and carboxyl surface groups are thought to contribute to their favorable biodistribution and biocompatibility. Beyond these physicochemical properties, only one mechanistic study has demonstrated the activation of the cep-1/p53 signaling pathway, leading to DNA damage-mediated germline apoptosis and *egl-1* induction [19].

In *D. melanogaster*, the only mechanistic investigation suggested that the modest toxicity observed for cysteamine-modified CDs at 500 μg/mL resulted from ROS-mediated

oxidative stress, leading to DNA damage, micronucleus formation, and nuclear fragmentation, with limited effects on survival and behavior [136].

4. Discussion

As demonstrated by the results presented in Figure 4A, 56% of the studies employed hydrothermal synthesis, highlighting it as the main strategy for the production of CQDs through green synthesis among the 102 studies evaluated in this review. This finding can be explained by the simplicity of the technique [24,31], which involves low operational costs and, more importantly, high compatibility with plant-derived biomass [19,26]. This approach enables the conversion of natural compounds rich in carbohydrates, lignin, proteins, and phenolic compounds into fluorescent nanostructures without using highly toxic reagents. As observed in the studies included in this review, hydrothermal synthesis has been successfully applied to medicinal plants [20], vegetables [15], microalgae [25], legumes [19], and biological residues [31], demonstrating the versatility of this method.

A wide variety of raw materials were identified, indicating that numerous carbon-rich biomass sources can be used for CQD production. Figure 4C shows that medicinal plants were the most frequently employed precursors [26], followed by fruits [38], vegetables, legumes [19] and microalgae [25]. This predominance may be attributed to the high concentration of secondary metabolites present in these materials, including flavonoids, phenolic compounds, amino acids, and sugars [19,26], which simultaneously promote the carbonization and functionalization of the nanoparticles. Furthermore, the use of these biomass sources reinforces the principles of the circular economy and green chemistry by adding value to renewable natural resources and low-cost residues [25,27].

Another important finding was that 76% of the solvents employed (Figure 5B) consisted of purified water, including distilled, deionized, and ultrapure water [24,31], demonstrating a growing trend toward the development of more sustainable synthetic protocols while reducing the use of organic solvents with potential toxic effects, such as formamide and other compounds commonly used in conventional synthesis routes [24]. In addition to being environmentally friendly, the use of water facilitates the extraction of hydrophilic biomolecules from biomass [87], contributing to the formation of oxygen-containing functional groups on CQDs surface, which are essential for their high dispersibility in aqueous media [31,87].

Regarding the experimental synthesis conditions, temperatures of approximately 200 °C were the most frequently reported (Figure 5B), mainly associated with reaction times of 4, 12, and 24 h (Figure 5A) [24]. These conditions may represent a balance between the efficiency of biomass carbonization and the preservation of the surface functional groups responsible for the colloidal stability of CQDs [10]. Lower temperatures may result in incomplete carbonization of the precursor, whereas higher temperatures tend to promote a greater degree of graphitization, significantly altering the structural and surface properties of nanoparticles [10,24].

The synthesis route, precursor selection, solvent, and purification procedures are parameters that may influence the biological and toxicological properties of CQDs. Green synthesis routes, particularly hydrothermal synthesis, may reduce the use of potentially toxic reagents and organic solvents, which may contribute to reducing the presence of potentially harmful residues [24]. In addition, the chemical composition of the precursor may influence the surface functional groups and physicochemical characteristics of the resulting CQDs, potentially affecting their interactions with biological systems [19,21]. The use of purified water as the reaction medium, as observed in most of the studies evaluated, may reduce the contribution of potentially hazardous organic solvents to the synthesis process [24]. Purification procedures, including dialysis and filtration, are also important

steps in the preparation of CQDs, although their specific contributions to the toxicological profile of the final material cannot be established from the available studies. Importantly, these factors should not be interpreted independently as determinants of CQD toxicity, as biological responses may also depend on the resulting physicochemical characteristics and the experimental conditions used in each biological model [19,28].

4.1. In Vivo Biosafety of Green-Synthesized CQDs

The unique physicochemical properties, surface functionality, and high biocompatibility of green-synthesized carbon quantum dots (CQDs) support their potential for in vivo therapeutic applications. Evidence links their biological effects to the modulation of oxidative stress and inflammatory responses. However, most studies treat these processes as secondary outcomes, and detailed evaluations of cellular signaling pathways remain limited. Classical biomarkers dominate, while more comprehensive molecular approaches and the relationship between CQD biodistribution and in vivo mechanisms are underexplored. Table S3 summarizes the information discussed below, in terms of species analyzed in terms of potential toxicity responses and the main applications evaluated using CQDs.

In terrestrial vertebrates, studies have generally reported no significant toxicity under the tested experimental conditions. These studies also demonstrated the potential of CQDs for bioimaging and therapeutic applications [49,55,64,68,72,86]. Biosafety assessment remains a fundamental component of nanomaterial development, and the establishment of appropriate safety standards is necessary to support their responsible use in biological and environmental systems [137]. Histopathology was the most frequently reported safety endpoint, and the absence of structural or morphological alterations in organs such as the liver, kidney, spleen, and heart supports the biocompatibility and low toxicity of green-synthesized CQDs under the investigated conditions [10,58,59]. Biochemical and hematological parameters, body weight, survival, and genotoxicity were evaluated less frequently but provided additional evidence supporting a favorable safety profile [28,58,59]. Collectively, these findings provide a basis for further investigation of CQD bioimaging and biodistribution in terrestrial vertebrate models [10,28,42,58,59].

Similarly, fish, particularly zebrafish, are well-established models for investigating nanobio interactions in aquatic environments. Standardized protocols and experimental tools enable reproducible assessments of CQD biocompatibility, nanotoxicity, and their biomedical applications [107,110,127]. The studies included in this review indicate that green-synthesized CQDs are effective fluorescent probes, showing broad tissue distribution and persistent fluorescence without relevant adverse effects under the evaluated bioimaging conditions [113,121,123,125]. These characteristics further support their potential for use in diagnostic imaging applications.

In invertebrate models, CQDs generally exhibit high in vivo biocompatibility. Approximately 90% of the reviewed studies reported no significant adverse effects on survival, development, morphology, or behavior, while also demonstrating effective fluorescence and bioimaging. The few adverse responses reported were dependent on the specific experimental conditions. In *C. elegans*, apoptosis occurs under light-activated photodynamic therapy conditions, representing a therapeutically induced response rather than evidence of intrinsic CQD toxicity [19]. In *D. melanogaster*, modest toxicity was observed only at the highest concentration tested (500 μg/mL), whereas the concentration used for bioimaging (250 μg/mL) did not produce such effects [136]. Overall, these findings suggest a broad safety margin for CQDs in invertebrate models, supporting their potential as fluorescent nanoprobes.

4.2. Bioimaging Applications of Green-Synthesized CQDs: Current Advances and Challenges

Despite exhibiting interesting properties as antioxidant nanoparticles, in the current scientific context, what appears to be most strongly evidenced, according to Figure 3 and Table S3, is their potential as a bioimaging sensor. As previously discussed, the main characteristics that draw attention to this applicability are their fluorescence and ease of water solubility, which do not appear to confer toxicity to organisms in vivo [22,23]. The evaluated outcomes highlight the ability of CQDs to incorporate into animal organs and cells, generating a fluorescent signal that can be easily tracked across a wide range of wavelengths [49–63].

Among the evaluated studies, the use of vertebrates such as rodents and zebrafish demonstrated that CQDs have a high capacity to cross biological barriers and distribute across different tissues, regardless of the route of exposure [69,108,121–126]. Among the barriers that can be crossed, the authors demonstrated the permeability of the chorion of zebrafish embryos by observing fluorescence originating from CQDs without any alteration in larval development [33,107,111,118], representing an alternative to other probes that may cause long-term inflammation.

In invertebrates, bioimaging outcomes provide a means to confirm CQD internalization [15,19]. In particular, the *C. elegans* model offers transparency that facilitates the observation of fluorescence and the permeability of CQDs and has been employed to assess both biosafety and bioimaging performance. Additionally, studies on invertebrates have shown that CQDs exhibit strong and stable multicolor fluorescence, which can be primarily internalized through the gastrointestinal tract and may subsequently spread to other tissues [15,131,134]. Nevertheless, it is important to note that only one of the studies evaluating bioimaging reported CQDs capable of affecting *D. magna* behavior at the highest concentration tested, although the nanomaterial had previously been surface-modified with cysteamine [38].

Overall, the evidence gathered across vertebrate and invertebrate models reinforces the reliability of green-synthesized CQDs as fluorescent nanoprobes capable of persistent, tissue-specific signals without compromising organismal viability, supporting their continued development for diagnostic imaging.

4.3. Therapeutic Applications of Green-Synthesized CQDs

Beyond bioimaging, the therapeutic potential of green-synthesized CQDs has garnered increasing attention [77,94,100]. Wound healing and tissue regeneration are among the most frequently investigated therapeutic applications, with studies reporting accelerated tissue repair, reduced inflammation, and enhanced bone recovery in different experimental models [48,53,70,79,87,88,90,93].

These effects appear to involve the modulation of oxidative stress, inflammatory responses, and regenerative processes [45,80,82,104]. Other, less frequently investigated applications include acute injury, neurological conditions, myocardial infarction, allergic rhinitis, and metabolic disorders, with studies reporting functional recovery and reduced tissue damage [54,90,97].

The diversity of therapeutic outcomes reported across biological models indicates that the effects of CQDs are unlikely to be explained by a single mechanism. Instead, the available evidence suggests the involvement of interconnected responses, particularly the modulation of oxidative status and inflammation, along with changes in cellular signaling pathways. Therefore, understanding these processes is therefore essential for interpreting both the therapeutic efficacy and potential adverse effects of green-synthesized CQDs.

4.4. General Mechanism of Biological Action of Green-Synthesized CQDs

Evidence from rodents, fish, and invertebrates indicates that oxidative stress modulation, inflammatory response modulation, and alterations in cell signaling pathways constitute the main mechanisms underlying the biological effects of green-synthesized CQDs in vivo. These mechanisms are rarely investigated as primary objectives; rather, they are frequently evaluated as secondary outcomes in biosafety and therapeutic studies [94,128,136]. Across biological models, these responses are associated with reduced inflammation at the wound site, accelerated tissue repair, and recovery of injured tissues, suggesting a combined contribution of oxidative stress modulation, inflammatory response modulation, and tissue regeneration [85,104]. The main mechanistic pathways and their interrelationships are summarized in Figure 9.

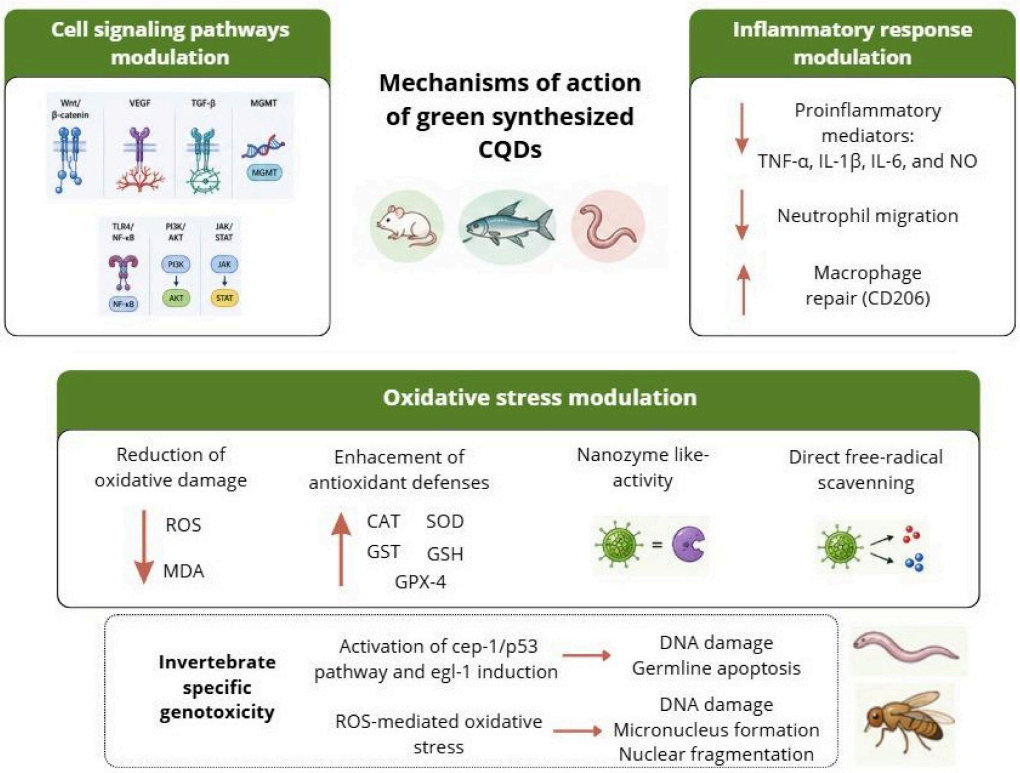

Figure 9. Overview of the main biological mechanisms associated with green-synthesized carbon quantum dots (CQDs) in in vivo models, including oxidative stress, inflammatory response, cell signaling, and invertebrate-specific genotoxic responses [19,44,79,80,87–91,104,127,129,136].

Oxidative stress modulation was the most frequently reported mechanism of action. CQD exposure was generally associated with reduced reactive oxygen species (ROS) and malondialdehyde (MDA) levels and increased antioxidant defenses, including catalase (CAT), glutathione-S-transferase (GST), and reduced glutathione (GSH), along with an increase in total antioxidant capacity (T-AOC) [44,45,53,85–87,94,96]. Deng et al. [127] further reported regulation of nitric oxide (NO) levels and increased expression of superoxide dismutase (SOD) and glutathione peroxidase 4 (GPX-4). CQDs may also exert antioxidant effects through nanozyme-like activity, mimicking antioxidant enzymes and promoting ROS removal [127], or through direct free radical scavenging, as reported in fish models [127,129]. In contrast, in invertebrate models, oxidative stress is also linked to genotoxic and apoptotic responses. In *C. elegans*, CQDs activate the cep-1/p53 pathway, leading to DNA damage-mediated germline apoptosis and egl-1 induction [19]. In *D. melanogaster*, the toxicity of cysteamine-modified CQDs is associated with ROS-mediated oxidative stress, DNA damage, micronucleus formation, and nuclear fragmentation [136].

In addition to the studies included in the present in vivo green synthesis dataset, carbon-dot-based platforms have been engineered as mechanistic tools to directly probe oxidative stress mediators. For instance, Wu et al. [138] developed a FRET-based ratiometric carbon-dot nanoprobe capable of selectively detecting peroxynitrite ($ONOO^-$) in live cells and in a drug-induced liver injury model, illustrating how carbon-dot systems can move beyond correlative biomarker measurements toward direct, real-time visualization of specific reactive species involved in oxidative and nitrosative stress pathways.

In parallel, inflammatory response modulation was observed across the studied models. CQDs reduced pro-inflammatory mediators, such as TNF-α, IL-1β, IL-6, and NO, while also decreasing neutrophil migration and increasing CD206 expression, a marker associated with repair macrophages [45,78,80,88,97,136]. Other studies have investigated cell signaling pathways, including Wnt/β-catenin, VEGF, TGF-β, MGMT, TLR4/NF-κB, PI3K/AKT, and JAK/STAT, and gut microbiota modulation [54,55,79,87,92,94].

Despite these advances, mechanistic investigations remain largely based on classical biomarkers, highlighting the limited use of comprehensive molecular approaches and the poorly understood relationship between CQD biodistribution and their in vivo mechanisms of action.

4.5. Future Directions and Challenges for Green-Synthesized CQDs

Finally, within the context of this review, we believe that it is appropriate to outline and discuss the future directions for the development of green-synthesized CQDs. First, the disparity between the knowledge generated regarding CQD characterization and application and studies focused on assessing potential toxic effects (Figure 2) is not novel. Kahru and Ivask [139] reported that for every thousand papers published in the field of nanotechnology, ten addressed toxicological aspects, whereas only one examined ecotoxicological responses. These figures are similar to those shown in Figure 2, where a preliminary analysis revealed that only 0.35% of studies evaluated the potential toxicity of CQDs.

Second, it is important to consider the issues and limitations previously discussed regarding nanosilver and other nanomaterials—particularly those produced via green synthesis—and to critically examine them; doing so can help avoid similar pitfalls in the development of CQDs. The study by Reijnders [140] raises the question of how "green" the so-called green synthesis methods are or whether the term is merely a label used in scientific titles without rigorous consideration of its application. The study noted that green synthesis research often employs highly energy-intensive processes, such as ultrasound- or microwave-assisted synthesis.

The twelve requirements for classifying a chemical synthesis as "green" were initially outlined by Anastas and Warner [141] to promote environmentally responsible practices and establish them as standard operating procedures. A recent study by Lipshutz and Handa [142] updated these principles by including a new principle that addresses the potential toxicity of a product. This new principle demands the development of metrics to evaluate the "greenness" of a process. In this context, the compilation of data on in vivo effects following exposure to CQDs presented in this review can be considered a necessary but insufficient step under the new principle proposed by Lipshutz and Handa [142]. Incorporating life cycle assessments (LCA), as noted by Reijnders [140] regarding nanosilver, makes it possible to identify environmentally costly processes, such as silver mining or the biomass production required for the synthesis deemed "green."

Ultimately, any approach to validating the "greenness" of a process must be grounded in metrics with a more holistic scope, such as LCA and E-factors. LCA studies, such as that by Fernandes et al. [143], concluded that an increase in quantum yield can offset the higher

environmental impact associated with certain carbon precursors used to produce quantum dots. Thus, both nanotoxicity and LCA information on CQDs are expected to contribute to a more precise selection of carbon nanomaterials that simultaneously present beneficial effects and low environmental impacts.

5. Conclusions

This review offers scientific information indicating that CQDs obtained via green synthesis have high biocompatibility, low toxicity, and great potential for application in bioimaging and therapy in different biological models. The results demonstrate that this class of carbon nanomaterials promotes promising therapeutic responses, mainly by modulating oxidative stress and the inflammatory response, even though the understanding of the molecular mechanisms remains limited.

Despite these advances, the predominance of short-term studies and the scarcity of pharmacokinetic and chronic toxicity assessments, as well as standardized synthesis and characterization protocols, make comparisons between studies difficult and limit their biomedical applications. To this end, future research should integrate long-term toxicological assessments, quantitative biodistribution, biological mechanisms, and life cycle analyses to provide robust information for the responsible, safe, and sustainable development of CQDs via green synthesis.

Finally, and considering the title of this article (Toxiciy of carbon quantum dots: Is there a dark side beyond its brighness?), the answer to the question seems to be that, based on the available evidence presented here, CQDs do not appear to be extremely toxic.

Supplementary Materials: The following supporting information can be downloaded at: https://www.mdpi.com/article/10.3390/coatings16091111/s1, Figure S1: Flowchart of the study identification, screening, eligibility, and inclusion process, prepared in accordance with the PRISMA 2020 guidelines; Figure S2: Overview of terrestrial vertebrates used in vivo studies included in this review. (A) Distribution of animal groups (mice, rats, and chickens) used for in vivo exposure to green-synthesized carbon quantum dots (CQDs). Frequency of mouse (B) and rat strains (C) employed in the included studies; Table S1: In vivo studies on green-synthesized carbon quantum dots (CQDs). Summary of the 102 studies evaluated, including species analyzed, exposure conditions, endpoints assessed, and toxicity/beneficial interpretation; Table S2: Frequency of DLS values in the analyzed articles; Table S3: Summary of the main effects, toxicity/safety profiles, and applications of green-synthesized carbon quantum dots (CQDs) across the in vivo biological models included in this review; Table S4: Main biological mechanisms evaluated as secondary or tertiary endpoints in terrestrial vertebrate models exposed in vivo to green-synthesized carbon quantum dots (CQDs).

Author Contributions: Conceptualization: M.M.d.S., L.V.d.C.N., M.d.C.V., V.d.S.M., L.Y.G.A., A.J.T.H., A.A., C.C., M.F.D. and J.M.M.; Methodology: M.M.d.S., A.J.T.H., A.A., M.d.C.V., L.V.d.C.N. and C.C.; Investigation: M.M.d.S., L.V.d.C.N., M.d.C.V., V.d.S.M., L.Y.G.A., A.J.T.H., A.A., C.C., M.F.D. and J.M.M.; Writing—original draft preparation: M.M.d.S., A.J.T.H., A.A., M.d.C.V. and J.M.M.; Writing—review and editing: M.M.d.S., L.V.d.C.N., M.d.C.V., V.d.S.M., L.Y.G.A., A.J.T.H., A.A., C.C., M.F.D. and J.M.M.; Supervision: J.M.M. and M.F.D.; Funding acquisition: J.M.M. All authors have read and agreed to the published version of the manuscript.

Funding: This research was funded by the Conselho Nacional de Desenvolvimento Científico e Tecnológico (CNPq), Brazil (Grant numbers PQ 308804/2025-2 and 353435/2025-2 awarded to José M. Monserrat and Carmen Costa, respectively) and by the Coordenação de Aperfeiçoamento de Pessoal de Nível Superior—Brasil (CAPES)—Finance Code 001, providing scholarships to Michel Machado Silva, Matheus de Castro Vieira, Victoria dos Santos Monteiro, and Lely Y. Guevara Argueta. A. Ayech and J.M. Monserrat acknowledge the support from Fundação de Amparo à Pesquisa do Estado do Rio Grande do Sul (FAPERGS, process 25/2551-0002624-5). J.M. Monserrat is grateful to INCT Nanocarbono e Materiais 2D (process number 408649/2024-0) for logistical and material support.

J.M. Monserrat and M.F. Desimone gratefully acknowledges the financial support provided by the CONICET–CNPq Bilateral Cooperation Program (CNPq process number 441451/2025-0 and Grant number CONICET 29520240100224CO, respectively).

Institutional Review Board Statement: Not applicable.

Informed Consent Statement: Not applicable.

Data Availability Statement: All data presented in this study are available in the Supplementary Materials.

Acknowledgments: Authors are grateful for the logistical and material support from Universidade Federal do Rio Grande—FURG. During the preparation of this study, the authors used Paper Pal (www.paperpal.com) to revise the English. Figure 1 was generated using the Gemini 3.6 Flash software. ChatGPT GPT-5.6 Luna (OpenAI) was used for figure organization (Figures 5–9 and layout standardization. After using these tools/services, the authors reviewed and edited the content as needed and took full responsibility for the publication's content.

Conflicts of Interest: The authors declare no conflicts of interest.

Abbreviations

CAT	Catalase
CD206	Cluster of Differentiation 206 (Marker of Reparative Macrophages)
CdSe	Cadmium selenide
CdTe	Cadmium telluride
CQDs	Carbon Quantum Dots
DLS	Dynamic Light Scattering
FRET	Förster Resonance Energy Transfer
GPX-4	Glutathione Peroxidase 4
GSH	Reduced Glutathione
GST	Glutathione-S-transferase
HO•	Hydroxil radical
IL-1β	Interleukin-1 beta
IL-6	Interleukin-6
JAK/STAT	Janus Kinase/Signal Transducer and Activator of Transcription
LCA	Life Cycle Assessment
MDA	Malondialdehyde
MGMT	O6-methylguanine-DNA methyltransferase
MWCO	Molecular Weight Cut-Off
NO	Nitric oxide
$ONOO^-$	Peroxynitrite
PI3K/Akt	Phosphoinositide 3-Kinase/Protein Kinase B
ROS	Reactive Oxygen Species
SOD	Superoxide Dismutase
TEM	Transmission Electron Microscopy
TGF-β	Transforming Growth Factor-beta
TLR4/NF-κB	Toll-like Receptor 4/Nuclear Factor kappa B
TNF-α	Tumor Necrosis Factor-alpha
UV	Ultraviolet
VEGF	Vascular Endothelial Growth Factor

References

1. Joudeh, N.; Linke, D. Nanoparticle classification, physicochemical properties, characterization, and applications: A comprehensive review for biologists. *J. Nanobiotechnol.* **2022**, *20*, 262. [CrossRef] [PubMed]
2. Khayal, A.; Dawane, V.; Amin, M.A.; Tirth, V.; Yadav, V.K.; Algahtani, A.; Khan, S.H.; Islam, S.; Yadav, K.K.; Jeon, B.-H. Advances in the Methods for the Synthesis of Carbon Dots and Their Emerging Applications. *Polymers* **2021**, *13*, 3190. [CrossRef] [PubMed]

3. Khalid, A.; Tomljenovic-Hanic, S. Emerging Fluorescent Nanoparticles for Non-Invasive Bioimaging. *Molecules* **2024**, *29*, 5594. [CrossRef] [PubMed]
4. Wang, L.; Ji, Y.; Chen, Y.; Zheng, S.; Wang, F.; Li, C. Recent research progress of fluorescence biosensors based on carbon dots in early diagnosis of diseases. *TrAC Trends Anal. Chem.* **2024**, *180*, 117962. [CrossRef]
5. Yang, L.; Hou, H.; Li, J. Frontiers in fluorescence imaging: Tools for the in situ sensing of disease biomarkers. *J. Mater. Chem. B* **2025**, *13*, 1133–1158. [CrossRef] [PubMed]
6. Xu, X.; Ray, R.; Gu, Y.; Ploehn, H.J.; Gearheart, L.; Raker, K.; Scrivens, W.A. Electrophoretic Analysis and Purification of Fluorescent Single-Walled Carbon Nanotube Fragments. *J. Am. Chem. Soc.* **2004**, *126*, 12736–12737. [CrossRef] [PubMed]
7. Hussen, N.H.; Hasan, A.H.; FaqiKhedr, Y.M.; Bogoyavlenskiy, A.; Bhat, A.R.; Jamalis, J. Carbon Dot Based Carbon Nanoparticles as Potent Antimicrobial, Antiviral, and Anticancer Agents. *ACS Omega* **2024**, *9*, 9849–9864. [CrossRef] [PubMed]
8. Al-Rasheidi, M.; Alabdulhadi, A.; Khan, F. Attaining a wide photoluminescence Stokes-shift of carbon dots obtained from waste biomass. *J. Mol. Struct.* **2025**, *1322*, 140627. [CrossRef]
9. Zhang, M.; Ma, Y.; Liao, F.; Shu, H.; Wu, Z.; Li, H.; Huang, H.; Huang, J.; Liu, Y.; Kang, Z. Chirality-Governed Anti-Aging Effects of Carbon Dots in Caenorhabditis Elegans. *Small* **2026**, *22*, e11386. [CrossRef] [PubMed]
10. Liu, Y.; Wang, X.; Wang, G.; Liu, B.; Zhang, X.; Chen, J.; Dou, H.; Zhao, L. Green biosynthesis of carbon quantum dots from lotus seed plumules for folic acid detection and bioimaging applications. *Spectrochim. Acta Part A Mol. Biomol. Spectrosc.* **2025**, *332*, 125825. [CrossRef] [PubMed]
11. Zhao, D.; Zhang, R.; Liu, X.; Li, X.; Xu, M.; Huang, X.; Xiao, X. Screening of Chitosan Derivatives-Carbon Dots Based on Antibacterial Activity and Application in Anti-*Staphylococcus aureus* Biofilm. *Int. J. Nanomed.* **2022**, *17*, 937–952. [CrossRef] [PubMed]
12. Chen, S.; Quan, Y.; Yu, Y.-L.; Wang, J.-H. Graphene Quantum Dot/Silver Nanoparticle Hybrids with Oxidase Activities for Antibacterial Application. *ACS Biomater. Sci. Eng.* **2017**, *3*, 313–321. [CrossRef] [PubMed]
13. Dube, E.; Okuthe, G.E. Applications of Antimicrobial Photodynamic Therapy in Aquaculture: Effect on Fish Pathogenic Bacteria. *Fishes* **2024**, *9*, 99. [CrossRef]
14. Wang, B.; Cai, H.; Waterhouse, G.I.N.; Qu, X.; Yang, B.; Lu, S. Carbon Dots in Bioimaging, Biosensing and Therapeutics: A Comprehensive Review. *Small Sci.* **2022**, *2*, 2200012. [CrossRef] [PubMed]
15. Singh, V.; Rawat, K.S.; Mishra, S.; Baghel, T.; Fatima, S.; John, A.A.; Kalleti, N.; Singh, D.; Nazir, A.; Rath, S.K.; et al. Biocompatible fluorescent carbon quantum dots prepared from beetroot extract for *in vivo* live imaging in *C. elegans* and BALB/c mice. *J. Mater. Chem. B* **2018**, *6*, 3366–3371. [CrossRef] [PubMed]
16. Amelia, M.; Lincheneau, C.; Silvi, S.; Credi, A. Electrochemical properties of CdSe and CdTe quantum dots. *Chem. Soc. Rev.* **2012**, *41*, 5728–5743. [CrossRef] [PubMed]
17. Shibu, E.S.; Hamada, M.; Nakanishi, S.; Wakida, S.; Biju, V. Photoluminescence of CdSe and CdSe/ZnS quantum dots: Modifications for making the invisible visible at ensemble and single-molecule levels. *Coord. Chem. Rev.* **2014**, *263–264*, 2–12. [CrossRef]
18. Gao, M.; Zhang, S.; Zhang, Z.; Wang, H.; Wu, J.; Chang, Z.; Zhang, Z.; Zhao, B. Comparison of toxic effects and underlying mechanisms of carbon quantum dots and CdSe quantum dots on *Chromochloris zofingiensis* from the chemical composition perspective. *Chemosphere* **2024**, *363*, 142911. [CrossRef] [PubMed]
19. Elsherbiny, S.M.; Shao, C.; Acheampong, A.; Khalifa, M.A.; Liu, C.; Huang, Q. Green synthesis of broccoli-derived carbon quantum dots as effective photosensitizers for the PDT effect testified in the model of mutant *Caenorhabditis elegans*. *Biomater. Sci.* **2022**, *10*, 2857–2864. [CrossRef] [PubMed]
20. Namdari, P.; Negahdari, B.; Eatemadi, A. Synthesis, properties and biomedical applications of carbon-based quantum dots: An updated review. *Biomed. Pharmacother.* **2017**, *87*, 209–222. [CrossRef] [PubMed]
21. Barve, K.; Singh, U.; Yadav, P.; Bhatia, D. Carbon-based designer and programmable fluorescent quantum dots for targeted biological and biomedical applications. *Mater. Chem. Front.* **2023**, *7*, 1781–1802. [CrossRef]
22. Molaei, M.J. Carbon quantum dots and their biomedical and therapeutic applications: A review. *RSC Adv.* **2019**, *9*, 6460–6481. [CrossRef] [PubMed]
23. Moradialvand, Z.; Parseghian, L.; Rajabi, H.R. Green synthesis of quantum dots: Synthetic methods, applications, and toxicity. *J. Hazard. Mater. Adv.* **2025**, *18*, 100697. [CrossRef]
24. Kong, J.; Wei, Y.; Zhou, F.; Shi, L.; Zhao, S.; Wan, M.; Zhang, X. Carbon Quantum Dots: Properties, Preparation, and Applications. *Molecules* **2024**, *29*, 2002. [CrossRef] [PubMed]
25. Suresh, U.; Sivaramakrishnan, S. Marine red algae-derived carbon quantum dots: A sustainable approach for mosquitocidal and antibacterial applications. *J. Ind. Eng. Chem.* **2026**, *154*, 409–426. [CrossRef]
26. Atchudan, R.; Jebakumar Immanuel Edison, T.N.; Perumal, S.; Vinodh, R.; Lee, Y.R. Multicolor-emitting carbon dots from Malus floribunda and their interaction with *Caenorhabditis elegans*. *Mater. Lett.* **2020**, *261*, 127153. [CrossRef]

27. Cong, S.; Liu, K.; Qiao, F.; Song, Y.; Tan, M. Biocompatible fluorescent carbon dots derived from roast duck for *in vitro* cellular and *in vivo C. elegans* bio-imaging. *Methods* **2019**, *168*, 76–83. [CrossRef] [PubMed]
28. Fu, C.; Qin, X.; Zhang, J.; Zhang, T.; Song, Y.; Yang, J.; Wu, G.; Luo, D.; Jiang, N.; Bikker, F.J. *In vitro* and *in vivo* toxicological evaluation of carbon quantum dots originating from *Spinacia oleracea*. *Heliyon* **2023**, *9*, e13422. [CrossRef] [PubMed]
29. Chen, Y.-C.; Chen, H.-H.; Lin, H.-J.; Huang, C.-C.; Chen, K.-F.; Peng, Y.-P.; Tsang, Y.F.; Chen, Y.-H.; Lin, K.-Y.A.; Lin, C.-H. Hepatotoxicity evaluations of different surface charged carbon quantum dots *in vivo* and *in vitro*. *Colloids Surf. B Biointerfaces* **2024**, *234*, 113760. [CrossRef] [PubMed]
30. Pourmadadi, M.; Rahmani, E.; Rajabzadeh-Khosroshahi, M.; Samadi, A.; Behzadmehr, R.; Rahdar, A.; Ferreira, L.F.R. Properties and application of carbon quantum dots (CQDs) in biosensors for disease detection: A comprehensive review. *J. Drug Deliv. Sci. Technol.* **2023**, *80*, 104156. [CrossRef]
31. Ahlawat, J.; Henriquez, G.; Varela-Ramirez, A.; Fairman, R.; Narayan, M. Gelatin-derived carbon quantum dots mitigate herbicide-induced neurotoxic effects *in vitro* and *in vivo*. *Biomater. Adv.* **2022**, *137*, 212837. [CrossRef] [PubMed]
32. Diab, E.A.; Ghali, M.; Mosaad, M.M. *In vitro* antimicrobial and anticancer potentials of green synthesized luminescent carbon quantum dots derived from artichoke leaves. *Sci. Rep.* **2025**, *15*, 16199. [CrossRef] [PubMed]
33. Yadav, P.; Benner, D.; Varshney, R.; Kansara, K.; Shah, K.; Dahle, L.; Kumar, A.; Rawal, R.; Gupta, S.; Bhatia, D. Dopamine-Functionalized, Red Carbon Quantum Dots for *In Vivo* Bioimaging, Cancer Therapeutics, and Neuronal Differentiation. *ACS Appl. Bio Mater.* **2024**, *7*, 3915–3931. [CrossRef] [PubMed]
34. Yang, S.-T.; Wang, X.; Wang, H.; Lu, F.; Luo, P.G.; Cao, L.; Meziani, M.J.; Liu, J.-H.; Liu, Y.; Chen, M.; et al. Carbon Dots as Nontoxic and High-Performance Fluorescence Imaging Agents. *J. Phys. Chem. C* **2009**, *113*, 18110–18114. [CrossRef] [PubMed]
35. Cheng, H.; Yang, C.; Xu, W.; Deng, Z.; Guan, G.; Zahid, H.; Liu, Y.; Hu, B.; Qin, Z.; Ren, M. Green synthesis of carbon quantum dots from *Euglena gracilis* for antibacterial and bioimaging applications. *Front. Nanotechnol.* **2025**, *7*, 1634916. [CrossRef]
36. Yan, H.; Li, P.; Wen, F.; Xu, Q.; Guo, Q.; Su, W. Green synthesis of carbon quantum dots from plant turmeric holds promise as novel photosensitizer for *in vitro* photodynamic antimicrobial activity. *J. Mater. Res. Technol.* **2023**, *22*, 17–34. [CrossRef]
37. Chung, C.-Y.; Chen, Y.-J.; Kang, C.-H.; Lin, H.-Y.; Huang, C.-C.; Hsu, P.-H.; Lin, H.-J. Toxic or Not Toxic, That Is the Carbon Quantum Dot's Question: A Comprehensive Evaluation with Zebrafish Embryo, Eleutheroembryo, and Adult Models. *Polymers* **2021**, *13*, 1598. [CrossRef] [PubMed]
38. Costa, R.S.; De Castro, M.O.; Da Silva, G.H.; Delite, F.D.S.; Strauss, M.; Ferreira, O.P.; Martinez, D.S.T.; Viana, B.C. Carbon-dots from babassu coconut (*Orbignya speciosa*) biomass: Synthesis, characterization, and toxicity to *Daphnia magna*. *Carbon Trends* **2021**, *5*, 100133. [CrossRef]
39. Pansari, P.; Sahu, S.; Alam, A.; Gupta, P.K.; Mishra, M.; Durga, G. Rational design and *in vivo* toxicity assessment of multichannel fluorescent carbon dots derived from Withania coagulans in *Drosophila melanogaster*. *Microchim. Acta* **2025**, *192*, 585. [CrossRef] [PubMed]
40. Li, M.; Zhang, C.; Mao, W.; Jiang, W. Carbon quantum dots modification reduces TiO_2 nanoparticle toxicity in an aquatic food chain. *J. Hazard. Mater.* **2025**, *486*, 137115. [CrossRef] [PubMed]
41. Azizah, R.N.; Verheyen, G.R.; Shkedy, Z.; Van Miert, S. Overview of *in vitro-in vivo* extrapolation approaches for the risk assessment of nanomaterial toxicity. *NanoImpact* **2024**, *35*, 100524. [CrossRef] [PubMed]
42. Huang, G.; Chen, X.; Wang, C.; Zheng, H.; Huang, Z.; Chen, D.; Xie, H. Photoluminescent carbon dots derived from sugarcane molasses: Synthesis, properties, and applications. *RSC Adv.* **2017**, *7*, 47840–47847. [CrossRef]
43. Xu, K.; Wang, Z.; Cui, M.; Jiang, Y.; Li, C.; Wang, Z.; Li, L.; Jia, C.; Zhang, L.; Wu, F. Turning Waste into Treasure: Functionalized Biomass-Derived Carbon Dots for Superselective Visualization and Eradication of Gram-Positive Bacteria. *Adv. Sci.* **2025**, *12*, 2411084. [CrossRef] [PubMed]
44. Yang, H.; Qiu, H.; Shan, J.; Nie, C.; Lin, Y.; Shen, Y.; Wang, X. Waste tobacco leaf-driven carbon dot nanozymes with high reactive oxygen species scavenging and anti-inflammatory activities for the amelioration of acute lung injury. *Ind. Crops Prod.* **2025**, *229*, 120958. [CrossRef]
45. Luo, T.; Li, M.; Tan, F.; Zhou, F.; Zhang, A.; Ruan, J.; Zhang, S.; Sun, Y.; Ding, K. Moutan cortex-derived CDs as ROS scavengers and natural p-STAT3 activity suppressor for inflammatory disease therapy. *Mater. Today Adv.* **2026**, *29*, 100703. [CrossRef]
46. Yang, Z.; Yin, T.; Wang, C.; Zhu, G.; Bai, L.; Jiang, Z.; Zhang, W. Biomass-derived carbon dots with pharmaceutical activity as temozolomide carrier for synergistic treatment of melanoma. *Bioorg. Chem.* **2025**, *164*, 108919. [CrossRef] [PubMed]
47. Zhang, M.; Zhao, Y.; Cheng, J.; Liu, X.; Wang, Y.; Yan, X.; Zhang, Y.; Lu, F.; Wang, Q.; Qu, H. Novel carbon dots derived from *Schizonepetae Herba Carbonisata* and investigation of their haemostatic efficacy. *Artif. Cells Nanomed. Biotechnol.* **2018**, *46*, 1562–1571. [CrossRef] [PubMed]
48. Ren, G.; Zhang, W.; Tang, Y.; Zhong, B.; Ming, L.; Fan, Q.; Huang, J.; Liu, H.; Li, Z.; Luo, P.; et al. Antibacterial activity and wound healing promotion of biomass carbon dots derived from a forestry pest, *Glenea cantor* (Coleoptera: Cerambycidae). *Chem. Biol. Technol. Agric.* **2025**, *12*, 128. [CrossRef]

49. Jia, Q.; Zheng, X.; Ge, J.; Liu, W.; Ren, H.; Chen, S.; Wen, Y.; Zhang, H.; Wu, J.; Wang, P. Synthesis of carbon dots from *Hypocrella bambusae* for bimodel fluorescence/photoacoustic imaging-guided synergistic photodynamic/photothermal therapy of cancer. *J. Colloid Interface Sci.* **2018**, *526*, 302–311. [CrossRef] [PubMed]
50. Hu, Y.-F.; Chen, Y.-X.; Chen, S.-Y. Green synthesis of near-infrared carbon dots as a novel aptamer-based fluorescence probe for the detection and imaging of alpha-fetoprotein. *Microchim. Acta* **2025**, *192*, 179. [CrossRef] [PubMed]
51. Anthony, A.M.; Murugan, R.; Subramanian, R.; Selvarangan, G.K.; Pandurangan, P.; Dhanasekaran, A.; Sohrab, A. Ultra-radiant photoluminescence of glutathione rigidified reduced carbon quantum dots (r-CQDs) derived from ice-biryani for *in vitro* and *in vivo* bioimaging applications. *Colloids Surf. A Physicochem. Eng. Asp.* **2020**, *586*, 124266. [CrossRef]
52. Srivastava, S.K.; Pratap, R.; Yadav, M.; Mishra, M.; Chaudhary, S.; Chawla, R.; Verma, A.K.; Parmar, A.S. Biogenic synthesis of highly stable multifluorescent, multifaceted carbon quantum dots as dual probe sensor for detection of heavy toxic metal ions—Fe^{3+} and As^{3+} in water and mouse fibroblast cell line NIH-3T3, and for live *in-vivo* imaging in mice. *Colloids Surf. A Physicochem. Eng. Asp.* **2025**, *723*, 137336. [CrossRef]
53. Dong, Z.; Yin, J.; Zhou, X.; Li, S.; Fu, Z.; Liu, P.; Shen, L.; Shi, W. Natural and biocompatible dressing unit based on tea carbon dots modified core-shell electrospun fiber for diabetic wound disinfection and healing. *Colloids Surf. B Biointerfaces* **2023**, *226*, 113325. [CrossRef] [PubMed]
54. Dong, L.; Zhao, Y.; Luo, J.; Li, X.; Wang, S.; Li, M.; Zou, P.; Kong, H.; Wang, Q.; Zhao, Y.; et al. Carbon Dots Derived from *Curcumae* Radix and Their Heartprotective Effect. *Int. J. Nanomed.* **2024**, *19*, 3315–3332. [CrossRef] [PubMed]
55. Marouzi, S.; Darroudi, M.; Hekmat, A.; Sadri, K.; Kazemi Oskuee, R. One-pot hydrothermal synthesis of carbon quantum dots from Salvia hispanica L. seeds and investigation of their biodistribution, and cytotoxicity effects. *J. Environ. Chem. Eng.* **2021**, *9*, 105461. [CrossRef]
56. Das, B.; Pal, P.; Dadhich, P.; Dutta, J.; Dhara, S. *In Vivo* Cell Tracking, Reactive Oxygen Species Scavenging, and Antioxidative Gene Down Regulation by Long-Term Exposure of Biomass-Derived Carbon Dots. *ACS Biomater. Sci. Eng.* **2019**, *5*, 346–356. [CrossRef] [PubMed]
57. Khan, H.R.; Yasmeen, H.; Tahir, M.A.; Kiani, A.F.; Munir, I.; Qamar, U.; Janiad, S.; Mahmood, S. Biofunctional and ecotoxicological assessment of *Rosa indica* derived nitrogen-doped Carbon Dots: A new frontier for sustainable nanomaterials. *Biocatal. Agric. Biotechnol.* **2025**, *69*, 103744. [CrossRef]
58. Sarkar, S.; Raghavan, A.; Deshpande, S.; Nayak, V.L.; Misra, S.; Sistla, R.; Ghosh, S. Valorization of Yellow Oleander to Nitrogen Doped Carbon Dots: Theragnostic and Genotoxicity Assessment. *ChemistrySelect* **2023**, *8*, e202203993. [CrossRef]
59. Lee, D.H.; So, E.; Mustafa, F.E.; Jeong, J.; Lee, B.-K. Preliminary Study on the Development of a Biodegradable Functional Nasal Packing Material. *Polymers* **2025**, *17*, 1878. [CrossRef] [PubMed]
60. Ding, H.; Zhou, X.; Qin, B.; Zhou, Z.; Zhao, Y. Highly fluorescent near-infrared emitting carbon dots derived from lemon juice and its bioimaging application. *J. Lumin.* **2019**, *211*, 298–304. [CrossRef]
61. Krishnaiah, P.; Atchudan, R.; Gangadaran, P.; Perumal, S.; Rajendran, R.L.; Sundramoorthy, A.K.; Suresh Kumar, R.; Ramalingam, S.; Ahn, B.-C.; Lee, S.W.; et al. A sustainable synthesis and applications of biomass waste-derived tunable fluorescent carbon dots: *In vitro* and *in vivo* fluorescent imaging. *J. Photochem. Photobiol. A Chem.* **2025**, *458*, 115944. [CrossRef]
62. Chang, D.; Zhao, Z.; Niu, W.; Shi, L.; Yang, Y. Iron ion sensing and *in vitro* and *in vivo* imaging based on bright blue-fluorescent carbon dots. *Spectrochim. Acta Part A Mol. Biomol. Spectrosc.* **2021**, *260*, 119964. [CrossRef] [PubMed]
63. Ji, X.; Wang, S.; Luo, Y.; Yuan, X.; Wei, Y.; Zhang, Q.; Qin, K.; Tu, Y. Green synthesis of weissella-derived fluorescence carbon dots for microbial staining, cell imaging and dual sensing of vitamin B12 and hexavalent chromium. *Dye. Pigment.* **2021**, *184*, 108818. [CrossRef]
64. Zhang, A.; Wang, Y.; Sui, X.; Xie, T.; Zhang, J.; Huang, Y.; Men, Y.; Zhang, P.; Chen, J. Renal-Clearable Biomass-Derived Carbon Dots with Red Fluorescence for Masked Cryptic Kidney Injury Imaging. *ACS Appl. Bio Mater.* **2025**, *8*, 1148–1156. [CrossRef] [PubMed]
65. Zhang, X.; Wang, H.; Ma, C.; Niu, N.; Chen, Z.; Liu, S.; Li, J.; Li, S. Seeking value from biomass materials: Preparation of coffee bean shell-derived fluorescent carbon dots via molecular aggregation for antioxidation and bioimaging applications. *Mater. Chem. Front.* **2018**, *2*, 1269–1275. [CrossRef]
66. Zheng, X.; Qin, K.; He, L.; Ding, Y.; Luo, Q.; Zhang, C.; Cui, X.; Tan, Y.; Li, L.; Wei, Y. Novel fluorescent nitrogen-doped carbon dots derived from *Panax notoginseng* for bioimaging and high selectivity detection of Cr^{6+}. *Analyst* **2021**, *146*, 911–919. [CrossRef] [PubMed]
67. Shi, W.; Li, J.; Pu, J.; Cheng, G.; Liu, Y.; Xiao, S.; Cao, J. Epigynum auritum-Derived Near-Infrared Carbon Dots for Bioimaging and Antimicrobial Applications. *Molecules* **2025**, *30*, 422. [CrossRef] [PubMed]
68. Tu, Y.; Wang, S.; Yuan, X.; Wei, Y.; Qin, K.; Zhang, Q.; Chen, X.; Ji, X. A novel fluorescent nitrogen, phosphorus-doped carbon dots derived from *Ganoderma lucidum* for bioimaging and high selective two nitrophenols detection. *Dye. Pigment.* **2020**, *178*, 108316. [CrossRef]

69. Srinivasan, D.; Balakrishnan, R.; Subbarayan, R.; Shrestha, R.; Chauhan, A.; Balasekar, P. Biocompatible PEGylated Carbon Quantum Dots Synthesized From Citrus Peel: Evaluation of Cell-Tracer Activity and *In Vivo* Imaging Potential. *J. Nanotechnol.* **2026**, *2026*, 5516948. [CrossRef]
70. Li, M.; Xu, M.; Su, W.; Zhao, F.; Hao, M.; Wang, H.; Yue, H.; Zhu, Q.; Li, W.; Wan, R.; et al. Biomass-derived fluorescent carbon dots from *Ginkgo biloba* leaves: A dual-functional nanomaterial for bioimaging and diabetic wound healing. *Chem. Eng. J.* **2025**, *526*, 171461. [CrossRef]
71. Khan, B.; Zhang, J.; Durrani, S.; Wang, H.; Nawaz, A.; Durrani, F.; Ye, Y.; Wu, F.-G.; Lin, F. Carbon-Dots-Mediated Improvement of Antimicrobial Activity of Natural Products. *ACS Appl. Mater. Interfaces* **2024**, *16*, 47257–47269. [CrossRef] [PubMed]
72. Khan, B.; Wang, H.; Wang, Y.; Latif, F.; Chen, P.; Han, M.; Feng, K.; Ye, Y.; Wu, F.-G.; Lin, F. Natural-product-derived carbon dots to combat *Candida albicans* infections without drug resistance by multifaceted antifungal mechanisms. *Chem. Eng. J.* **2025**, *523*, 168622. [CrossRef]
73. Li, M.; Xie, Z.; Zheng, M. Bioinspired carbon dots/curcumin nanocomposite films: Synergistic antibacterial-antioxidant dual action for precision therapy of infected burn wounds. *Colloids Surf. A Physicochem. Eng. Asp.* **2026**, *733*, 139295. [CrossRef]
74. Sheng, L.; Wang, Z.; Song, L.; Yang, X.; Ye, Y.; Sun, J.; Ji, J.; Geng, S.; Ning, D.; Zhang, Y.; et al. Antimicrobial carbon dots/pectin-based hydrogel for promoting healing processes in multidrug-resistant bacteria-infected wounds. *Int. J. Biol. Macromol.* **2024**, *264*, 130477. [CrossRef] [PubMed]
75. Zhang, Y.; Jia, Q.; Ge, J. Thea Viridis derived carbon dots for drug-resistant bacterial infections by photodynamic therapy. *Chin. J. Lumin.* **2023**, *44*, 1112–1120. [CrossRef]
76. Lv, J.; Tian, H.; Pan, L.; Chen, Z.; Li, M.; Ghiladi, R.A.; Qin, Z.; Yin, X. Biomass derived carbon dots with antibacterial and anti-inflammatory properties for the treatment of wound healing. *Chem. Eng. Sci.* **2024**, *295*, 120084. [CrossRef]
77. Qi, J.; Zhang, T.; Zhang, R.; Liu, J.; Zong, M.; Zhang, Q.; Ping, Y.; Gong, Y.; Zhang, B.; Liu, X.; et al. Fe-doped herbal medicine-based carbon dots nanozyme as safe and effective antimicrobial and wound healing agent. *Sustain. Mater. Technol.* **2024**, *41*, e01087. [CrossRef]
78. Wen, F.; Su, W.; Cen, L.; Chen, Y.; Huo, L.; Zhong, H.; Li, P. Natural fluorescent carbon quantum dots embedded polyvinyl alcohol/chitosan film with photoregulation and high antibacterial efficiency for infected wound healing. *Int. J. Biol. Macromol.* **2025**, *306*, 141716. [CrossRef]
79. Guo, S.; Tong, J.; Liu, Y.; Qin, D.; Yan, J.; Peng, H.; Sun, L.; Jing, X.; Wu, X.; Li, B. Synthesis of Eucommia ulmoides-derived carbon dots for anti-inflammatory and accelerated wound healing. *Int. Immunopharmacol.* **2024**, *143*, 113606. [CrossRef] [PubMed]
80. Li, J.; Fu, W.; Zhang, X.; Zhang, Q.; Ma, D.; Wang, Y.; Qian, W.; Zhu, D. Green preparation of ginger-derived carbon dots accelerates wound healing. *Carbon* **2023**, *208*, 208–215. [CrossRef]
81. Murugesan, S.; Srinivasan, V.; Lakshmanan, D.K.; Venkateswaran, M.R.; Jayabal, S.; Muthukumar Nadar, M.S.A.; Kathiravan, A.; Asha Jhonsi, M.; Thilagar, S.; Periyasamy, S. Evaluation of the anti-rheumatic properties of thymol using carbon dots as nanocarriers on FCA induced arthritic rats. *Food Funct.* **2021**, *12*, 5038–5050. [CrossRef] [PubMed]
82. Shakiba-Marani, R.; Ehtesabi, H. A flexible and hemostatic chitosan, polyvinyl alcohol, carbon dot nanocomposite sponge for wound dressing application. *Int. J. Biol. Macromol.* **2023**, *224*, 831–839. [CrossRef] [PubMed]
83. Dong, X.; Yan, W.; Zhang, D.; Dong, X.; Li, Y. Biomass spinach-drived metal-free carbon dots-based nanozyme for multimodal nitrite sensing and functionalized by glucose oxidase as ROS amplifiers to enhance tumor therapy. *Int. J. Biol. Macromol.* **2025**, *304*, 140875. [CrossRef] [PubMed]
84. Jia, R.; Liu, P.; Gong, Y.; Gao, Y.; Xiong, Y.; Song, X.; Peng, J.; Lan, M.; Shi, X. PH-responsive doxorubicin-loaded Artemisia argyi carbon dots: Enhanced targeted therapy for hepatocellular carcinoma. *RSC Adv.* **2025**, *15*, 37645–37659. [CrossRef] [PubMed]
85. Xue, M.; Zhao, J.; Zhan, Z.; Zhao, S.; Lan, C.; Ye, F.; Liang, H. Dual functionalized natural biomass carbon dots from lychee exocarp for cancer cell targetable near-infrared fluorescence imaging and photodynamic therapy. *Nanoscale* **2018**, *10*, 18124–18130. [CrossRef] [PubMed]
86. Yang, Q.; Liu, J.; Cai, W.; Liang, X.; Zhuang, Z.; Liao, T.; Zhang, F.; Hu, W.; Liu, P.; Fan, S.; et al. Non-heme Iron Single-Atom Nanozymes as Peroxidase Mimics for Tumor Catalytic Therapy. *Nano Lett.* **2023**, *23*, 8585–8592. [CrossRef] [PubMed]
87. Liu, Z.-F.; Wang, J.-H.; Wang, C.-P.; Wang, Q.; Li, J.; Han, C.-J.; Lu, Z. Green hydrothermal valorization of *Rosa damascena* Mill. Floral waste into functional carbon dots for anti-inflammatory nanomedicine. *Ind. Crops Prod.* **2025**, *236*, 122115. [CrossRef]
88. Li, Y.; Li, Q.; Zhu, Y.; Huang, C.; Li, H.; Deng, Z.; Xu, C.; Wang, W.; Chen, L.; Zhang, S.; et al. Medicinal Plant-Derived Carbon Dots Nanozymes Ameliorate Ulcerative Colitis via Anti-inflammatory, Antioxidant, and Gut Barrier-Protective Effects. *ACS Appl. Mater. Interfaces* **2025**, *17*, 42751–42766. [CrossRef] [PubMed]
89. Wu, T.; Bai, X.; Zhang, Y.; Dai, E.; Ma, J.; Yu, C.; He, C.; Li, Q.; Yang, Y.; Kong, H.; et al. Natural medicines-derived carbon dots as novel oral antioxidant administration strategy for ulcerative colitis therapy. *J. Nanobiotechnol.* **2024**, *22*, 511. [CrossRef] [PubMed]
90. Li, X.; Lu, Y.; Li, J.; Zhou, S.; Wang, Y.; Li, L.; Zhao, F. Photoluminescent carbon dots (PCDs) from sour apple: A biocompatible nanomaterial for preventing UHMWPE wear-particle induced osteolysis via modulating Chemerin/ChemR23 and SIRT1 signaling pathway and its bioimaging application. *J. Nanobiotechnol.* **2022**, *20*, 301. [CrossRef] [PubMed]

91. Hong, H.-S.; Park, H.-J.; Lee, J.-M.; Chen, Z.-Y.; Kim, T.-W.; Seo, Y.-S.; Kang, J.-W.; Seo, Y.-K. Bioactive Carbon Dots from Clove Residue: Synthesis, Characterization, and Osteogenic Properties. *Biomedicines* **2025**, *13*, 527. [CrossRef] [PubMed]
92. Shi, X.-F.; Jia, X.-L.; Wu, Z.-F.; Zhang, Y.; Chen, X.-P.; Xiong, H.-M.; Mao, Y.-Q. Carbon dots derived from ginger for inhibiting inflammatory osteolysis. *Nanoscale* **2025**, *17*, 27269–27280. [CrossRef] [PubMed]
93. Guo, Z.; Wang, Z.; Liu, Y.; Wu, H.; Zhang, Q.; Han, J.; Liu, J.; Zhang, C. Carbon Dots from Lycium barbarum Attenuate Radiation-Induced Bone Injury by Inhibiting Senescence via METTL3/Clip3 in an m6 A-Dependent Manner. *ACS Appl. Mater. Interfaces* **2023**, *15*, 20726–20741. [CrossRef] [PubMed]
94. Wang, L.; Li, Z.-Y.; Zhong, C.-L.; Teng, Z.-Y.; Wang, B.; Rehman, A.; Han, L.-W.; Zeng, K.-W.; Zhang, J.-G.; Lu, Z.-Y. Therapeutic potential of naturally derived carbon dots in sepsis-associated acute kidney injury. *Chin. Med.* **2025**, *20*, 49. [CrossRef] [PubMed]
95. Yang, L.; Dai, F.; Tang, H.; Li, M.; An, Y.; Tan, Y.; Liu, R.; Tan, X.; Zhang, W.; Askari Rizvi, S.F.; et al. Lophatherum-Gracile driven near-infrared carbon dots inhibit ferroptosis and mitophagy to treat acute kidney injury. *Chem. Eng. J.* **2025**, *513*, 162637. [CrossRef]
96. Wang, X.; Wu, T.; Yang, Y.; Zhou, L.; Wang, S.; Liu, J.; Zhao, Y.; Zhang, M.; Zhao, Y.; Qu, H.; et al. Ultrasmall and highly biocompatible carbon dots derived from natural plant with amelioration against acute kidney injury. *J. Nanobiotechnol.* **2023**, *21*, 63. [CrossRef] [PubMed]
97. Dong, L.; Zhang, H.; Wang, K.; Wang, C.; Wu, Y.; Shao, W.; Liu, K.; Lan, X.; Han, J.; Cheng, J.; et al. Carbon Dots Extracted from the Plant *Gardenia jasminoides* Ameliorates Ischemia–Reperfusion Injury. *Pharmaceuticals* **2025**, *18*, 870. [CrossRef] [PubMed]
98. Xu, G.; Wang, J.; Hou, G.; Wang, X.; Xu, Y.; Tian, J.; Ding, Y. Marine-derived carbon dots: A safe and effective solution for noise-induced hearing loss. *J. Nanobiotechnol.* **2026**, *24*, 387. [CrossRef] [PubMed]
99. Huang, Y.; Li, M.; Dong, L.; He, C.; Zou, P.; Xia, M.; Jin, B.; Wang, S.; Lu, Z.; Qu, H.; et al. Crinis Carbonisatus-Derived Carbon Dot Suspension Alleviates Temporal Lobe Epilepsy. *Pharmaceuticals* **2025**, *18*, 1481. [CrossRef] [PubMed]
100. Lin, S.; Zheng, Y.; Xu, Y.; Zhou, Y.; He, X.; Zhang, C.; Yuan, C. Hawthorn carbon dots: A novel therapeutic agent for modulating body weight and hepatic lipid profiles in high-fat diet-fed mice. *Nanoscale* **2025**, *17*, 2668–2681. [CrossRef] [PubMed]
101. Sun, Z.; Lu, F.; Cheng, J.; Zhang, M.; Zhu, Y.; Zhang, Y.; Kong, H.; Qu, H.; Zhao, Y. Hypoglycemic Bioactivity of Novel Eco-Friendly Carbon Dots Derived from Traditional Chinese Medicine. *J. Biomed. Nanotechnol.* **2018**, *14*, 2146–2155. [CrossRef] [PubMed]
102. Chen, R.; Ma, H.; Li, X.; Wang, M.; Yang, Y.; Wu, T.; Zhang, Y.; Kong, H.; Qu, H.; Zhao, Y. A Novel Drug with Potential to Treat Hyperbilirubinemia and Prevent Liver Damage Induced by Hyperbilirubinemia: Carbon Dots Derived from *Platycodon grandiflorum*. *Molecules* **2023**, *28*, 2720. [CrossRef] [PubMed]
103. Han, B.; Shen, L.; Xie, H.; Huang, Q.; Zhao, D.; Huang, X.; Chen, X.; Li, J. Synthesis of Carbon Dots with Hemostatic Effects Using Traditional Chinese Medicine as a Biomass Carbon Source. *ACS Omega* **2023**, *8*, 3176–3183. [CrossRef] [PubMed]
104. Zhou, L.; Yang, Y.; Li, T.; Zhao, Y.; Yuan, J.; He, C.; Huang, Y.; Ma, J.; Zhang, Y.; Lu, F.; et al. Green carbon dots derived from *Zingiberis Rhizoma Carbonisatum* alleviate ovalbumin-induced allergic rhinitis. *Front. Immunol.* **2024**, *15*, 1492181. [CrossRef] [PubMed]
105. Peng, H.; Zeng, X.; Li, S.; Wang, X. A Novel Cortex Phellodendri Chinensis-Based Carbon Dots Platform for Remarkable Analgesia for Clinical Pain Management. *Vet. Med. Sci.* **2024**, *10*, e70090. [CrossRef] [PubMed]
106. Huang, Y.; Zhou, X.; Zhou, R.; Zhang, H.; Kang, K.; Zhao, M.; Peng, Y.; Wang, Q.; Zhang, H.; Qiu, W. One-Pot Synthesis of Highly Luminescent Carbon Quantum Dots and Their Nontoxic Ingestion by Zebrafish for *In Vivo* Imaging. *Chem. Eur. J.* **2014**, *20*, 5640–5648. [CrossRef] [PubMed]
107. Yao, Y.-Y.; Gedda, G.; Girma, W.M.; Yen, C.-L.; Ling, Y.-C.; Chang, J.-Y. Magnetofluorescent Carbon Dots Derived from Crab Shell for Targeted Dual-Modality Bioimaging and Drug Delivery. *ACS Appl. Mater. Interfaces* **2017**, *9*, 13887–13899. [CrossRef] [PubMed]
108. Abu, N.; Chinnathambi, S.; Kumar, M.; Etezadi, F.; Bakhori, N.M.; Zubir, Z.A.; Md Salleh, S.N.; Shueb, R.H.; Karthikeyan, S.; Thangavel, V.; et al. Development of biomass waste-based carbon quantum dots and their potential application as non-toxic bioimaging agents. *RSC Adv.* **2023**, *13*, 28230–28249. [CrossRef] [PubMed]
109. Kumar, M.; Chinnathambi, S.; Bakhori, N.; Abu, N.; Etezadi, F.; Thangavel, V.; Packwood, D.; Sivaniah, E.; Pandian, G.N. Biomass-derived carbon dots as fluorescent quantum probes to visualize and modulate inflammation. *Sci. Rep.* **2024**, *14*, 12665. [CrossRef] [PubMed]
110. Malavika, V.; Rajan, M.R.; Krishnamoorthi, R.; Adithya, K.C.; Kim, K. Citrus-Derived Carbon Quantum Dots: Synthesis, Characterization, and Safety Evaluation in Zebrafish (*Danio rerio*) for Potential Biomedical and Nutritional Applications. *Micro* **2025**, *5*, 50. [CrossRef]
111. Kowsalya, P.; Bharathi, S.U.; Chamundeeswari, M. Photocatalytic treatment of textile effluents by biosynthesized photo-smart catalyst: An eco-friendly and cost-effective approach. *Environ. Dev. Sustain.* **2023**, *26*, 10719–10739. [CrossRef]
112. Tungare, K.; Bhori, M.; Racherla, K.S.; Sawant, S. Synthesis, characterization and biocompatibility studies of carbon quantum dots from *Phoenix dactylifera*. *3 Biotech* **2020**, *10*, 540. [CrossRef] [PubMed]

113. Kim, K.W.; Oh, G.-W.; Jung, S.-H.; Ko, S.-C.; Kim, J.-Y.; Yang, D.; Jo, D.-M.; Lee, D.-S.; Choi, G. Simple Fabrication and Biological Evaluation of Ulva australis-Derived Marine Carbon Dots with Anti-Inflammation, Anti-Oxidation, and Anti-Adipogenesis Features. *J. Mar. Sci. Eng.* **2025**, *13*, 1878. [CrossRef]
114. Shi, J.; Zhou, Y.; Ning, J.; Hu, G.; Zhang, Q.; Hou, Y.; Zhou, Y. Prepared carbon dots from wheat straw for detection of Cu2+ in cells and zebrafish and room temperature phosphorescent anti-counterfeiting. *Spectrochim. Acta Part A Mol. Biomol. Spectrosc.* **2022**, *281*, 121597. [CrossRef] [PubMed]
115. Wang, Y.; Gu, Z.; Dong, J.; Zhu, J.; Liu, C.; Li, G.; Lu, M.; Han, J.; Cao, S.; Chen, L.; et al. Correction: Green synthesis of chlorella-derived carbon dots and their fluorescence imaging in zebrafish. *RSC Adv.* **2024**, *14*, 14505. [CrossRef] [PubMed]
116. Zhu, W.; Gao, X.; Yu, X.; Li, Q.; Zhou, Y.; Qiu, H.; Xing, B.; Zhang, Z. Screening of multifunctional fruit carbon dots for fluorescent labeling and sensing in living immune cells and zebrafishes. *Microchim. Acta* **2022**, *189*, 223. [CrossRef] [PubMed]
117. Manjubaashini, N.; Bargavi, P.; Balakumar, S. Carbon quantum dots derived from agro waste biomass for pioneering bioanalysis and *in vivo* bioimaging. *J. Photochem. Photobiol. A Chem.* **2024**, *454*, 115702. [CrossRef]
118. Ren, H.; Yuan, Y.; Labidi, A.; Dong, Q.; Zhang, K.; Lichtfouse, E.; Allam, A.A.; Ajarem, J.S.; Wang, C. Green process of biomass waste derived fluorescent carbon quantum dots for biological imaging *in vitro* and *in vivo*. *Chin. Chem. Lett.* **2023**, *34*, 107998. [CrossRef]
119. Shao, R.; Abbas, K.; Osipov, V.Y.; Zhu, H.; Li, Y.; Usama; Bi, H. Red-emitting carbon dots prepared from Epipremnum Aureum leaves extract for biological imaging. *Acta Phys.-Chim. Sin.* **2026**, *42*, 100134. [CrossRef]
120. Zhao, W.; Zhang, Y.; Cao, B.; Li, Z.; Sun, C.; Cao, X.; Cong, S. Characteristics of Mussels-Derived Carbon Dots and Their Applications in Bio-Imaging and Detection of Riboflavin. *Foods* **2022**, *11*, 2451. [CrossRef] [PubMed]
121. Perumal, S.D.M.; Thangaian, D.T.; Nandhakumar, M.; Devaraj, N.; Kalagatur, N.K. Evolution of large stokes shift and non-radiative energy transfer phenomenon in sustainable blue-fluorescent CQDs upon subnanomolar detection of Acebrophylline. *Spectrochim. Acta Part A Mol. Biomol. Spectrosc.* **2025**, *329*, 125559. [CrossRef] [PubMed]
122. Wang, Y.; Gu, Z.; Dong, J.; Liu, C.; Zhu, J.; Wang, Z.; Li, J.; Lu, M.; Han, J.; Cao, S.; et al. Synthesis of biosafe spirulina-derived carbon dots and their fluorescence imaging in zebrafish. *Results Chem.* **2025**, *16*, 102503. [CrossRef]
123. Dias, C.; Vasimalai, N.; Sárria, M.P.; Pinheiro, I.; Vilas-Boas, V.; Peixoto, J.; Espiña, B. Biocompatibility and Bioimaging Potential of Fruit-Based Carbon Dots. *Nanomaterials* **2019**, *9*, 199. [CrossRef] [PubMed]
124. Liu, Y.; Tang, Y.; Xu, Q.; Cao, Y.; Wei, J.; Liang, Z.; Jiang, X.; Wu, Y.; Guo, C. Solvothermal regulation of fluorescence quantum yield of carbon dots derived from biomass for zebrafish imaging. *J. Lumin.* **2024**, *271*, 120583. [CrossRef]
125. Zhang, J.-H.; Niu, A.; Li, J.; Fu, J.-W.; Xu, Q.; Pei, D.-S. *In vivo* characterization of hair and skin derived carbon quantum dots with high quantum yield as long-term bioprobes in zebrafish. *Sci. Rep.* **2016**, *6*, 37860. [CrossRef] [PubMed]
126. Li, W.; Zeng, G.; Yan, J.; Liu, X.; Jiang, X.; Yang, J.; Liu, J.; Sun, D. One-pot green synthesis of I@CNDs-Fe3O4 hybrid nanoparticles from kelp for multi-modal imaging *in vivo*. *Mater. Sci. Eng. C* **2021**, *124*, 112037. [CrossRef] [PubMed]
127. Deng, W.; Zang, C.; Li, Q.; Sun, B.; Mei, X.; Bai, L.; Shang, X.; Deng, Y.; Xiao, Y.; Ghiladi, R.A.; et al. Hydrothermally Derived Green Carbon Dots from *Broccoli* Water Extracts: Decreased Toxicity, Enhanced Free-Radical Scavenging, and Anti-Inflammatory Performance. *ACS Biomater. Sci. Eng.* **2023**, *9*, 1307–1319. [CrossRef] [PubMed]
128. Praseetha, P.K.; Vibala, B.V.; Sreedevy, K.; Vijayakumar, S. Aloe-vera conjugated natural carbon quantum dots as bio-enhancers to accelerate the repair of chronic wounds. *Ind. Crops Prod.* **2021**, *174*, 114152. [CrossRef]
129. Zhu, H.; Li, Y.; Qin, W.; Usama; Lou, Y.; Jiang, L.; Cai, H.; Ge, Z.; Abbas, K.; Li, Z.; et al. Beyond the Source: Nanozyme-like Carbon Dots Derive from Cherry Tomato Mitigate Ocular Oxidative Stress. *ACS Appl. Bio Mater.* **2025**, *8*, 10405–10418. [CrossRef] [PubMed]
130. Atchudan, R.; Jebakumar Immanuel Edison, T.N.; Perumal, S.; Lee, Y.R. Indian Gooseberry-Derived Tunable Fluorescent Carbon Dots as a Promise for *In Vitro*/*In Vivo* Multicolor Bioimaging and Fluorescent Ink. *ACS Omega* **2018**, *3*, 17590–17601. [CrossRef]
131. Atchudan, R.; Jebakumar Immanuel Edison, T.N.; Shanmugam, M.; Perumal, S.; Somanathan, T.; Lee, Y.R. Sustainable synthesis of carbon quantum dots from banana peel waste using hydrothermal process for *in vivo* bioimaging. *Physica E Low.-Dimens. Syst. Nanostruct.* **2021**, *126*, 114417. [CrossRef]
132. He, Y.; Chen, X.; Wang, P.; Li, X.; Wang, B.; Wang, X.; Wu, Z.; Wang, W. One-step green synthesis of carbon dots derived from *Plumeria alba* flowers for sensing and bioimaging. *New J. Chem.* **2023**, *47*, 8877–8884. [CrossRef]
133. Karuppasamy, B.D.; Perumal, S.; Atchudan, R.; Sundramoorthy, A.K.; Manoj, D.; Sambasivam, S.; Karthik, N.; Kamaraj, E.; Suresh Kumar, R.; Ramalingam, S.; et al. Eco-friendly *Coccinia* Grandis-derived excitation-dependent fluorescence of carbon dots for *In-Vivo* bioimaging and fluorescent ink applications. *Mater. Sci. Eng. B* **2024**, *303*, 117300. [CrossRef]
134. Karuppasamy, B.D.; Perumal, S.; Atchudan, R.; Sundramoorthy, A.K.; Ramalingam, S.; Manoj, D.; Babu, R.S.; Park, J.H.; Lee, S.W. Cornus Officinalis-derived hydrophilic carbon dots with Regulatable emission for *in-vivo* imaging with good biocompatibility. *Inorg. Chem. Commun.* **2025**, *182*, 115350. [CrossRef]

135. Prathap, N.; Balla, P.; Shivakumar, M.S.; Periyasami, G.; Karuppiah, P.; Ramasamy, K.; Venkatesan, S. *Prosopis juliflora* hydrothermal synthesis of high fluorescent carbon dots and its antibacterial and bioimaging applications. *Sci. Rep.* **2024**, *13*, 9676. [CrossRef] [PubMed]
136. Pansari, P.; Sahu, S.; Mishra, M.; Gupta, P.K.; Durga, G. *In-vivo* toxicological study of cysteamine modified carbon dots derived from *Ruellia simplex* on fruit fly for potential bioimaging. *Biocatal. Agric. Biotechnol.* **2024**, *61*, 103359. [CrossRef]
137. Fadeel, B.; Farcal, L.; Hardy, B.; Vázquez-Campos, S.; Hristozov, D.; Marcomini, A.; Lynch, I.; Valsami-Jones, E.; Alenius, H.; Savolainen, K. Advanced tools for the safety assessment of nanomaterials. *Nat. Nanotechnol.* **2018**, *13*, 537–543. [CrossRef] [PubMed]
138. Wu, Y.; Sun, L.-L.; Han, H.-H.; He, X.-P.; Cao, W.; James, T.D. Selective FRET nano probe based on carbon dots and naphthalimide–isatin for the ratiometric detection of peroxynitrite in drug-induced liver injury. *Chem. Sci.* **2024**, *15*, 757–764. [CrossRef] [PubMed]
139. Kahru, A.; Ivask, A. Mapping the Dawn of Nanoecotoxicological Research. *Acc. Chem. Res.* **2013**, *46*, 823–833. [CrossRef] [PubMed]
140. Reijnders, L. Is 'Green' Gold and Silver Nanoparticle Synthesis Environmentally Friendly? *Nanomaterials* **2025**, *15*, 1095. [CrossRef] [PubMed]
141. Anastas, P.T.; Warner, J.C. *Green Chemistry: Theory and Practice*; Oxford University Press: Oxford, UK, 2000. [CrossRef]
142. Lipshutz, B.H.; Handa, S. Modernizing the 12 principles of green chemistry: It's time. *Green Chem.* **2026**, *28*, 5606–5612. [CrossRef]
143. Fernandes, S.; Esteves Da Silva, J.C.G.; Pinto Da Silva, L. Comparative life cycle assessment of high-yield synthesis routes for carbon dots. *NanoImpact* **2021**, *23*, 100332. [CrossRef] [PubMed]